GEOLOGICAL SURVEY OF CANADA
COMMISSION GEOLOGIQUE DU CANADA

Open File 3614

ANALYSIS OF GRAVITY AND MAGNETIC HORIZONTAL-GRADIENT VECTOR DATA OVER THE BURIED TRANS-HUDSON OROGEN AND CHURCHILL-SUPERIOR BOUNDARY ZONE IN SOUTHERN SASKATCHEWAN AND MANITOBA

By

H.V. Lyatsky, J.R. Dietrich and D.J. Edwards

Geological Survey of Canada (Calgary), 3303 - 33 Street N.W.
Calgary, Alberta T2L 2A7

JULY 1998

SUMMARY

Reprocessing and interpretation of regional gravity and aeromagnetic data from southeastern Saskatchewan and southwestern Manitoba is undertaken as part of a study of basement-sedimentary cover relationships in the Williston sedimentary basin in Canada. This report presents the results of horizontal-gradient vector (HGV) processing of gridded gravity and aeromagnetic data, and an interpretation of Precambrian basement trends and domains.

The HGV method resolves potential-field anomalies in more detail than do many other data enhancement techniques. In HGV maps, the horizontal gradient of the gravity or magnetic field is treated as a vector, having both a direction and magnitude. The gradient is represented on a map as an arrow with an origin at a grid node. Varying the arrow polarity (uphill or downhill - towards or away from local maxima in the potential field) and scaling (linear or logarithmic) provides for a suite of HGV displays, each of which presents a visually unique image of potential-field anomaly fabric.

HGV patterns within the study area are highly variable and include linear and curvilinear anomalies of varying orientations, circular and ovoid anomalies occurring singly and in clusters, and polygonal anomalies of varying sizes. These patterns indicate crystalline basement beneath this part of the Williston Basin is composed of a complex mosaic of crustal belts, plutons, faults and fault-bounded blocks.

The analysis of HGV-processed potential-field data provides new insights into the crustal structure and tectonic fabric of the Archean Superior Province, Proterozoic Trans-Hudson Orogen, and intervening Churchill-Superior boundary zone beneath the northern Williston basin. East-west and north-south aligned potential-field anomalies outline the main Kenoran (2.8-2.4 Ga) and Hudsonian (1.9-1.8 Ga) age crustal fabrics, respectively. In magnetic HGV maps, the transition from E-W-trending (Superior Province) to N-S-trending (Churchill Province) crustal fabrics commonly appears gradational or irregular, suggesting the Churchill-Superior "boundary zone" within the study area is broad and structurally segmented. In gravity HGV maps, a prominent N-S aligned belt of ovoid-shaped anomalies appears to provide a regionally consistent potential-field signature for part of the boundary zone. The Tabbernor fault zone in the central Trans-Hudson Orogen can be identified in magnetic HGV maps, but is not readily apparent in gravity maps.

INTRODUCTION

The Williston Basin has substantial proven and potential oil and gas resources. In many parts of the basin, the development of hydrocarbon traps and migration pathways was influenced by basement structures (eg. Osadetz et al., 1989; Gerhard and Anderson, 1990; Potter and St.Onge, 1991; Gibson, 1995). To evaluate basement-sedimentary cover relationships on a regional basis (and, by extension, implications for hydrocarbon exploration), geophysical mapping of basement trends beneath the basin is required. In this report we present preliminary interpretations of basement tectonic domains and structures beneath the northeastern Williston Basin, based on horizontal-gradient vector (HGV) processing of public-domain gravity and aeromagnetic data.

The study area covers some 120,000 km^2 of southeastern Saskatchewan and southwestern Manitoba (49 ° to 52 ° N latitude, 99 ° to 104 ° W longitude; Fig. 1). The thickness of Phanerozoic sedimentary strata (and depth to basement) increases in a SW direction across the study area, from a few hundred metres in the northeast corner to over 3000 metres in the southwest corner. Precambrian crystalline basement beneath this part of the Williston Basin consists of parts of two major crustal provinces and their boundary zone: the Archean Superior Province to the east, the Archean-Early Proterozoic Churchill Province and Trans-Hudson Orogen to the west, and the intervening Churchill-Superior boundary zone. The Early Proterozoic Trans-Hudson Orogen, which developed during the ~1.9-1.8 Ga Hudsonian Orogeny (Hoffman, 1988; Lewry and Stauffer, eds., 1990), and adjacent Archean Hearne Province are constituent parts of the broader Churchill tectonic province (Fig.1). The Tabbernor fault zone is a N-S trending fault system in the core of the Trans-Hudson Orogen. The Churchill-Superior boundary zone is a complex transition zone between the Superior Province (that has a predominantly E-W fabric and has been stable since the Kenoran orogeny) and the eastern Churchill Province (Trans-Hudson Orogen), a region with a more variable fabric that was molded by the Hudsonian orogeny (Green et al., 1979; Weber, 1990).

The subsurface locations of these crustal elements were mapped in the 1970s and 1980s through extrapolation of potential-field and other geophysical signatures from exposed Precambrian Shield areas in northern Saskatchewan and Manitoba southward beneath the Williston Basin (Green et al., 1979, 1985; Klasner and King, 1986; Thomas et al., 1987). At the time of these early studies, potential-field data coverage was incomplete in many parts of southern Saskatchewan and Manitoba. Recent studies incorporating newer, broader coverage potential-field datasets include interpretations of regional Precambrian basement domains in Saskatchewan (Miles, Stone and Thomas, 1997), and mapping of Trans-Hudson Orogen crustal domains adjacent to the southern margin of the Canadian Shield in east-central Saskatchewan and west-central Manitoba (Leclair et al., 1997). For this study, we incorporate the currently available gravity and aeromagnetic data for southeastern Saskatchewan and southwestern Manitoba, and extensively utilize the HGV method for data enhancement. The resulting interpretations of the nature and distribution of Precambrian crustal elements within the study area are more detailed than presented in previous publications.

Data Base

The potential-field data used in this study are part of Geological Survey of Canada's National Gravity and Aeromagnetic Database, publicly available through the Geophysical Data Centre, GSC Ottawa.

The existing gravity coverage across southern Saskatchewan and Manitoba is fairly uniform, with station spacing averaging about 10 km over most of the region (approximately 1 station per township). In some areas adjacent to the Canada-U.S. border, gravity measurements are more tightly spaced at 3 to 4 km intervals. In a few localities, small gaps of 20 to 30 km occur in the gravity coverage. Magnetic coverage across the study area encompasses data from numerous aeromagnetic surveys, of varying vintages and acquisition parameters. Aeromagnetic data were acquired along E-W survey lines, with line spacing varying from 1600 to 3200 m in older (1960s) surveys to 800 m in more recent (1990s) surveys. Flight altitudes (mean terrain clearance) varied from 305 m to 975 m in older surveys to 150 m in recent surveys. Approximately half of the magnetic data set within the study area is derived from 1990s surveys. Anomaly resolution loss due to wider line spacing in older surveys is minimized in the study area, because the older data occur primarily in southwestern parts of the region where depth to basement is the greatest. Magnetic anomaly maps derived from the merged magnetic datasets reveal no discernible artifacts or edge effects associated with original survey acquisition boundaries (at the time this study was undertaken, a small gap in magnetic coverage existed in one location in the southeastern part of the study area - the area of missing data is represented by a blank area in the HGV-processed magnetic maps).

In this study, we use Bouguer gravity and IGRF-reduced total-field magnetic data (Figs. 2 and 3). For the magnetic data, there was no reduction to the pole applied prior to HGV processing. This was considered unnecessary because the study area lies at a high magnetic latitude where the geomagnetic field is steep (~75°; Newitt and Haines, 1990). In addition, reduction to the pole would have introduced an undesirable side-effect of artificially altering remanent-magnetization components of the magnetic anomalies (the correction assumes rock magnetization is entirely induced). In well-studied parts of the exposed Canadian Shield, the measured remanent magnetization of some rock samples is close to and even exceeds the induced magnetization (Sprenke et al., 1986).

HORIZONTAL-GRADIENT VECTOR (HGV) PROCESSING

The HGV method of processing potential-field data was proposed originally by Lyatsky et al. (1990) as a technique to enhance subtle anomalies. The first published applications of this method were from studies of the Queen Charlotte Basin offshore British Columbia, and the Peace River Arch region of Alberta (Lyatsky et al., 1992 a,b). In these studies, HGV processing of public-domain GSC data helped resolve patterns of basement faults and plutons. In a more recent study of the central Alberta part of the Western Canada Sedimentary Basin, Edwards et al. (1996) integrated HGV-processed potential-field data with well-data information to infer basement controls on Phanerozoic geology.

Distinctiveness of the HGV method from more conventional methods of computing the horizontal gradient (eg. Sharpton et al., 1987; Goodacre et al., 1987) is two-fold. First, and most important, unlike conventional methods where the horizontal gradient of a potential field is treated as a scalar having a magnitude only, the HGV technique recognizes it fully as a vector quantity having a magnitude and a direction. The meaning of the horizontal gradient can be understood by considering a potential-field anomaly map in terms of relief. The direction of the gradient is perpendicular to the amplitude contours, and the gradient's magnitude is the "steepness" of the slope in that direction. At a point on a map, the horizontal gradient is represented by an arrow whose length is proportional to the gradient magnitude and whose pointed direction is the direction of the gradient. The second

difference in the HGV technique from other horizontal gradient methods is achieved by fitting a third-order surface to a 5x5 window of potential-field grid nodes, rather than a planar (first-order) surface as is usually done. This improves the quality of the fit and thus the fidelity of the computed magnitude and direction of the gradient. A window of 5x5 data points is centered on each grid node for which the gradient is calculated. Inside the window, a third-order surface fitted to the 25 data points is assumed to represent the anomaly relief and the parameters of this surface are used to compute the horizontal gradient at the window centre. The 5x5 window size was chosen originally (Sharpton et al., 1987; Goodacre et al., 1987) in part because a 3x3 window may be too small to "see" anomaly shapes properly and would give undue weight to spurious data values. On the other hand, a 7x7 or larger window results in the undesirable averaging of data from a large area around the grid node.

Gridding Interval for HGV Processing

In this study, we use 2-km gridded magnetic data and 2- and 5-km gridded gravity data. The 2-km grid interval was considered optimal, given the original data acquisition parameters and the scope of geological investigations. The 5-km gridded gravity data set was included to evaluate the effects of grid-cell size on HGV output. Tighter gridding intervals (even for sparsely recorded potential-field data) have been found experimentally to produce better resolution HGV maps. One reason for this is that a filtering paradox occurs with the use of a 5x5 window in computing the horizontal gradient at a grid node. Due to data averaging within the window, the window may act as a smoothing filter that suppresses short-wavelength anomalies - even though these are exactly the anomalies horizontal-gradient methods are intended to enhance. Reducing the grid interval reduces the size of the area encompassed by the window, thereby reducing this spatial-filtering effect. The fitting of a third-order surface to the data in the HGV method also reduces the smoothing problem, but does not eliminate it. Using a higher-order surface would reduce the smoothing even further, but would also introduce more sensitivity to data errors (Lyatsky et al., 1992b).

Figures 4 and 5 illustrate gravity HGV maps from 5-km gridded and 2-km gridded data, respectively. The tighter (2 km) gridded data provide for significantly improved anomaly definition, due to the increased number and closeness of the HGV arrows. A drawback in using tighter gridded datasets is that increased sample density requires more computer processing and storage capacity.

HGV Arrow Scaling

HGV arrows originate at grid nodes, and can be plotted either towards or away from the local maxima in the potential field ("uphill" or "downhill"). To help resolve anomaly details in complex or subdued anomaly domains, the length-scaling factors of the HGV arrows and the scaling method (linear or logarithmic) can be varied. In the original version of the HGV method (Lyatsky et al., 1990, 1992a,b), map arrows were scaled only linearly. This representation is attractively straightforward, but it has a drawback (particularly in the case of magnetic data) where the range of the gradient magnitudes is wide. In plots of linearly-scaled magnetic HGV data, long arrows from high-relief features extend into and often obscure the surrounding anomalies (Fig. 6). The problem of long arrows and data clutter can be alleviated by either arrow clipping or logarithmic scaling. In the clipping method (developed for this study), arrow lengths are clipped to a user-selected fraction of

the maximum value in the data set. Experimentation with clipping parameters and scaling factors (eg. Figs. 7, 8 and 9) can provide an optimal map in which arrow cluttering is minimized and anomaly shapes are resolved.

An alternative method to alleviate arrow cluttering is logarithmic scaling, which has the advantage (over clipping) of preserving the gradient magnitude information (eg. Fig. 10). Logarithmic scaling is one of two modifications to the HGV method developed by Thurston (1991). The other modification, published by Thurston and Brown (1994), and used by Edwards et al. (1996) and in this study, involves the use of a deconvolution-based polynomial-approximation computation to determine parameters of the best-fit third-order surface in a 5x5 window, which had previously been calculated using a least-squares technique. The logarithmic scaling technique has been upgraded in this study by eliminating several program deficiencies. Still, logarithmic scaling produces some undesirable artifacts that result from the mathematical nature of the logarithmic function itself. For example, the logarithm of a very small positive number ($<<1.0$) is a large negative number; the resulting artificial reversal of the gradient sign and HGV arrow direction is accounted for in data processing, but the high value of the logarithm itself creates a problem of having very small gradients represented by long HGV arrows. Similar distortions occur for gradient-magnitude values near 1.0, because the logarithm of 1.0 equals zero and these gradients are unrealistically scaled down. These artifacts are considerable for the gravity data, but less so for the magnetic data. The reason for this is that the gravity field in the study area is generally characterised by low relief, with an abundance of low (<1.0) gradient magnitudes, whereas the magnetic field is characterised by typically much higher gradient magnitudes. Logarithmically-scaled gravity HGV plots (Fig. 11) distort anomaly shapes and outlines, although they have some display value in enhancing anomaly "skeletons" (with artificially boosted arrows along near-flat anomaly crests and troughs).

Figures 12 to 19 illustrate a representative suite of gravity and magnetic HGV maps, with variable scaling and arrow polarity.

SOURCES OF GRAVITY AND MAGNETIC ANOMALIES IN THE STUDY AREA

An anomaly is the difference between observed gravity or magnetic values and the values that would be recorded if the Earth were laterally uniform (Nettleton, 1971). Gravity and magnetic anomalies reflect lateral variations in the density and magnetization of rocks. Specific rock-composition changes that generate potential-field anomalies can rarely be determined unequivocally, and the geologic significance of anomalies is usually the subject of interpretation.

Gravity Anomalies

Bulk density is the rock property whose variations relate a gravity anomaly to its geologic source. There is no precise correlation between density and rock type. Igneous and metamorphic crystalline rocks are generally denser than most sedimentary rocks, with mafic crystalline rocks typically of higher density than felsic ones. Lateral rock-density contrasts that produce gravity anomalies can occur at any level within, above or below the crystalline crust. Mantle-sourced density variations produce long-wavelength gravity anomalies that will not be well expressed in HGV maps.

For the Western Canada Sedimentary Basin, practical interpretation experience and quantitative

modelling studies (eg. Anderson et al., 1988) show that gravity anomalies from intra-basin density variations are typically small in amplitude. In the study-area data set, the vast majority of gravity anomalies reflect lateral density variations within the crystalline crust.

Magnetic Anomalies

Total magnetization is the rock property that relates a magnetic anomaly to its geologic source (Reynolds et al., 1990). The most common magnetic mineral is magnetite, and there is generally a correlation between rock magnetite content and its magnetic susceptibility. Magnetic minerals occur most commonly in igneous and metamorphic rocks, but there is no precise or consistent relationship between igneous/metamorphic rock type and magnetic susceptibility. Sedimentary rocks are generally less magnetic.

Magnetic anomalies recorded over the Western Canada Sedimentary Basin are usually attributed to crystalline basement sources (Ross et al., 1994a). In the Alberta part of the basin, examples have been documented of local occurrences of intra-basin magnetic anomaly sources, including igneous dykes and mineralized faults (Ross et al., 1994b; Peirce et al., 1997). Although intra-basin magnetic sources may be locally present in parts of the Williston Basin, the vast majority of magnetic anomalies in the study-area data set are believed to reflect lateral variations in the distribution of magnetic minerals within the uppermost part of the crystalline crust.

In the Canadian Shield, spatial variations in magnetic-mineral content generally mimic regional fabrics associated with Precambrian magmatism, metamorphism and ductile deformation (Sprenke et al., 1986). Although the lower boundary of the magnetic anomaly-generating lithospheric layer is defined by the Curie isotherm (generally, at mid-crustal depths), deep-seated magnetic sources produce long-wavelength magnetic anomalies (as measured at or near surface) that will not be not clearly expressed in magnetic HGV maps.

Common Potential-field Signatures

Detailed studies correlating gravity and magnetic data with geologic field maps and drill-core data in the western Canadian Shield have shown that linear and round potential-field anomalies are common signatures of basement fault zones and primary magmatic (plutonic) fabrics, respectively (Sprenke, et al. 1986; Leclair et al. 1997). Synthetic modelling tests have demonstrated that HGV-processed data are particularly useful for identifying and mapping faults, block edges, and plutons (Edwards and Lyatsky, 1996; Edwards, 1997). Block edges and faults are represented by linear HGV patterns, while plutons and other domal features are represented by radial HGV patterns.

DESCRIPTIONS OF POTENTIAL-FIELD ANOMALY PATTERNS AND DOMAINS IN THE STUDY AREA

Bouguer gravity anomaly values within the study area vary from -5 to -85 mGal (Fig. 2). Aeromagnetic anomaly values vary from -1000 to over +1500 nT (Fig. 3). The highest-amplitude magnetic anomaly within the region (between 99° and 100° W, near 50 ° N) is known from drill-core data to be associated with a Precambrian iron formation (C. McGregor and R. Bezys, written comm.,

1997).

In a regional perspective, similar anomaly fabrics are observed in the gravity and magnetic contour maps (Figs. 2 and 3). Major anomaly trends are E-W, NNE and N-S in southwestern Manitoba, and N-S and NNW in southeastern Saskatchewan. As defined in previous studies (Green et. al., 1979, 1985), E-W magnetic anomaly trends are characteristic of the Superior Province, and N-S magnetic anomaly trends are characteristic of the Churchill Province and Churchill-Superior boundary zone. In the study area, E-W anomaly trends are apparent in the southeastern and northeastern parts of the magnetic map, and southeastern part of the gravity map. North-trending magnetic and gravity anomalies are prevalent west of 101° W. The eastward transition from N-S to E-W trending magnetic anomalies commonly appears gradational or irregular. In previous studies, the location of the Churchill-Superior boundary zone was correlated to a "magnetic quiet zone", a series of magnetic lows extending across western Manitoba and North Dakota (Green et al., 1979, 1985; Klasner and King, 1986). Within the study area, the magnetic quiet zone is represented by several disconnected and irregular-shaped magnetic lows, located along or near 101° W longitude. Overall, the magnetic signature of this zone appears variable and complex.

In the western part of the study area (near 103°W longitude), a prominent change in the general character of the magnetic anomaly field is apparent: from relatively high-relief anomalies in the east to low-relief anomalies in the west. The boundary between these two magnetic domains lies on trend with the Tabbernor fault zone.

Gravity HGV Anomaly Domains

Two regional-scale anomaly domains are apparent in the gravity HGV maps (illustrated in Fig. 20). The gravity domain division is also apparent in the Bouguer gravity contour map (Fig. 2), but with less clarity than in the HGV maps.

Domain I (in the east) is characterised by a diffuse collection of circular and ovoid HGV anomalies, with little coherent regional fabric. A few linear anomalies with E-W and WNW trends occur in the southern and western parts of Domain I. In contrast, Domain II (in the west) is characterised by a pronounced anomaly fabric, expressed by N-S, NNW, and other less prevalent HGV anomaly trends. Linear HGV anomalies are significantly more abundant in Domain II than in Domain I. The eastern margin of Domain II is marked by a prominent N-S trending band of circular/ovoid anomalies (II-B in Fig. 20). This anomaly zone appears to be laterally offset in an E-W direction, near 51° N. A second N-S ovoid anomaly belt (II-C in Fig. 20) occurs in the central part of Domain II.

The long, linear gravity HGV anomalies are believed to be indicative of intra-basement faults or crustal block edges. The faults/block edges are commonly straight and vary in length from 10 to 90 km. In some areas, particularly in the western part of Domain II, linear anomaly segments outline polygonal blocks. Within them, consistent gravity HGV arrow directions may be indicative of crustal block tilt. For example, HGV arrows within the large NNW-striking crustal block (feature II-D in Fig. 20) indicate a WSW block tilt. The circular and ovoid gravity HGV anomalies are generally considered to be indicative of plutons and pluton clusters, with the II-B anomaly trend possibly marking a curvilinear pluton belt (magmatic arc?). The occasionally observed off-centre position of their apices (relative to the anomaly base) indicates some of the causative plutons may be asymmetric

or tilted. Ovoid gravity anomalies are both positive and negative (the former being more common), suggesting differences in pluton composition.

Magnetic HGV Anomaly Domains

Five major anomaly domains are apparent in the magnetic HGV maps (illustrated in Fig. 21). The domains are generally apparent in the total-field contour map (Fig. 3), but again with less clarity than in the HGV maps. Some HGV magnetic domain boundaries are abrupt, while others appear gradational. The locations of domain boundaries in some areas are only approximate.

Domain I, in the easternmost part of the study area, is characterised by a predominance of E-W trending linear magnetic anomalies. The E-W anomaly trends extend farther west in areas north of 51°N than in areas to the south. This apparent offset in the domain's western boundary occurs at the same latitude as the gravity II-B anomaly offset.

Domain II is characterised by variable anomaly patterns, including NNW- and NNE-trending ovoid anomaly clusters, and a single large ovoid anomaly feature (II-A in Fig. 21). Domain III, in the central part of the study area, is characterised by a mix of linear and ovoid anomalies, with a predominance of N-S, NNE and NNW trends. Conjugate sets of NW- and NE-trending anomalies are locally apparent in parts of this domain.

Domain IV, in the northwestern part of the study area, is characterised by a predominance of NNW trending linear anomalies. Although some anomaly orientations are similar to those in parts of Domain III, Domain IV is differentiated on the basis of a more subdued anomaly field and a reduction in the number of small ovoid anomalies (which occur in abundance in Domain III). Domain V, in the southwestern part of the study area, is characterised by a subdued magnetic anomaly field and lack of a dominant fabric. The south-central part of the domain contains a cluster of linear and ovoid anomalies with NNW and NW trends. The margins of Domain V are marked by NW- and NE-trending linear anomalies, with a particularly sharp contact at the southernmost domain III-V boundary.

As in the Canadian Shield, many of the long, linear magnetic HGV anomalies in the study area (eg. in domains IV and V) are probably associated with basement shear zones. Most of the ovoid magnetic HGV anomalies are probably associated with igneous plutons or batholiths. The ovoid anomalies are most commonly associated with magnetic highs. The large ovoid anomaly II-A (in Domain II) is probably associated with an igneous batholith, as mineral-exploration wells that penetrated the Precambrian basement within this anomaly area encountered granite and granodiorite (C. McGregor and R. Bezys, written comm., 1997). In the total-field magnetic contour map (Fig. 3), anomaly II-A appears as a broad, single feature, whereas the magnetic HGV maps show that the feature consists of numerous culminations.

INTERPRETATIONS OF CRUSTAL ARCHITECTURE

Churchill-Superior Boundary Zone

The areas of gravity Domain I and magnetic domains I and II are interpreted to be part of the Superior crustal province, while gravity Domain II and magnetic Domain III probably encompass the

Churchill-Superior boundary zone and eastern part of the Trans-Hudson Orogen. The north-trending, gravity II-B anomaly belt (Fig. 20) is a pronounced, regionally consistent feature that may provide the best signature of the Churchill-Superior boundary zone (or a part thereof) within the study area. This gravity anomaly trend can be traced NNE, beyond the study area to the Thompson Belt (Churchill-Superior boundary zone) within and adjacent to the exposed Canadian Shield (Fig. 22). Within the study area, the gravity II-B trend closely parallels the eastern margin of magnetic Domain III (Fig. 21).

The complexity of magnetic HGV patterns in the general area of the boundary zone suggest there may be considerable overlap and interpenetration of Superior (Kenoran) and Churchill (Hudsonian) tectonic fabrics. Both gravity and magnetic HGV patterrns indicate the boundary zone is probably segmented by transverse structures, including at least one major east- or northeast-trending feature near latitude 51° N.

Tabbernor Fault Zone

The most abrupt magnetic domain boundary within the study area is associated with the western margin of Domain III (Fig. 21). In detail, this domain boundary consists of at least three linear segments, each of different orientation (N-S, NNW, and NNE). These segments could represent strands of the Tabbernor fault zone. The along-strike variation in fault orientation may indicate complex or multi-phase tectonism. In the gravity data, Domain II contains many linear gravity HGV anomalies that are probably indicative of faults, but there is no single linear anomaly or anomaly zone that extends across the entire map area coincident with the magnetically-defined Tabbernor fault zone. Still, the gravity anomalies within this area generally follow the main N-S, NNW and NNE trends of the Tabbernor fault zone.

FUTURE STUDIES

HGV-processed potential-field data were used in this study to interpret Precambrian tectonic domains and structural trends beneath the northeastern Williston Basin. Some Precambrian features have undoubtedly influenced aspects of Phanerozoic development of the Williston Basin. An evaluation of linkages between gravity and magnetic signatures and Phanerozoic basin geology calls for detailed integration of potential-field, seismic and well-data information. Such analyses are the focus of ongoing studies (eg. Dietrich et al., 1997).

ACKNOWLEDGEMENTS

We thank the University of Calgary and Shell Canada Ltd. for providing access to computer facilities and processing/modelling software. The HGV processing software used in this study currently resides at the Department of Geology and Geophysics, University of Calgary. We thank L. Lawley and J. Janveau (GSC Ottawa) for providing initial gridded data files, M. Staniland and P. Neelands (GSC Calgary) for technical support, and G. Ross (GSC Calgary) for a review of the report.

REFERENCES

Anderson, N.L., Brown, R.J., and Hinds, R.C.
1988: Geophysical aspects of Wabamun salt distribution in southern Alberta. Canadian Journal of Exploration Geophysics, v.24, p.166-178.

Dietrich, J.R., Magnusson, D.H., Lyatsky, H.V., Hajnal, Z., and Redley, P.
1997: Basement-sedimentary cover relationships in the eastern Williston Basin. CSPG-SEPM 1997 Joint Convention, Calgary, Program with Abstracts, p.80.

Edwards, D.J.
1997: An integrated geophysical investigation of basement controls on Devonian carbonates in central Alberta. PhD thesis, Department of Geology and Geophysics, University of Calgary, 348p.

Edwards, D.J. and Lyatsky, H.V.
1996: Synthetic modelling of Bouguer gravity horizontal-gradient vector data. University of Calgary, Lithoprobe Newsletter, v.9, No.2. p.45-49.

Edwards, D.J., Lyatsky, H.V., and Brown, R.J.
1996: Interpretation of gravity and magnetic data using the horizontal-gradient vector method in the Western Canada Basin. First Break, v.14, no.6, p.231-246.

Gerhard, L.C. and Anderson, S.B.
1990: Petroleum geology of the Williston Basin. In; Interior Cratonic Basins, AAPG Memoir 51 (M.Leighton, D.Kolata, D. Oltz and J. Eidel, eds.), p. 507-559.

Gibson, R.I.
1995: Basement tectonics and hydrocarbon production in the Williston Basin: An intepretive overview. In; Proceedings of the Seventh International Williston Basin Symposium (L. Hunter and R. Schalla, eds.), p.3-9.

Goodacre, A.K., Grieve, R.A.F., Halpenny, J.F., and Sharpton, V.L.
1987: Horizontal Gradient of the Bouguer Gravity Anomaly Map of Canada. Geological Survey of Canada, Canadian Geophysical Atlas, Map 5.

Green, A.G., Cumming, G.L. and Cedarwall, D.
1979: Extension of the Churchill-Superior boundary zone into southern Canada. Canadian Journal of Earth Sciences, v.16, p.1691-1701.

Green, A.G., Hajnal, Z., and Weber, W.
1985: An evolutionary model of the western Churchill Province and western margins of the Superior Province in Canada and the north-central United States. Tectonophysics, v.116, p.281-322.

Hoffman, P.F.
1988: United Plates of America - Early Proterozoic assembly and growth of Laurentia. Annual Reviews of Earth and Planetary Interiors, v. 60, p.169-194.

Hood, P.J. and Teskey, D.J.
1989: Aeromagnetic gradiometer program of the Geological Survey of Canada, Geophysics, v.54, p.1012-1022.

Klasner, J.S. and King, E.R.
1986: Precambrian basement geology of North and South Dakota. Canadian Journal of Earth Science, v.23, p.1083-1102.

Leclair, A.D., Lucas, S.B., Broome, H.J., Viljoen, D.W., and Weber, W.

1997: Regional mapping of Precambrian basement beneath Phanerozoic cover in southeastern Trans-Hudson Orogen, Manitoba and Saskatchewan. Canadian Journal of Earth Sciences, v.34, p. 618-634.

Lewry, J.F. and Stauffer, M.R. (eds.)
1990: The Early Proterozoic Trans-Huson Orogen of North America. Geological Association of Canada, Special Paper 37.

Lucas, S.B., White, D., Bleeker, W., Hajnal, Z., Lewry, J. and Weber, W.
1996: Crustal structure of the Superior Boundary Zone (Thompson Belt) from new Lithoprobe seismic reflection data. In; Trans-Hudson Orogen Workshop, Lithoprobe Report 55, p.82-94.

Lyatsky, V.B., Brown, R.J., and Lyatsky, H.V.
1990: The use of potential-field horizontal gradient vector data in hydrocarbon exploration. Lyatsky Geoscience Research and Consulting Ltd., Calgary, 26p.

Lyatsky, H.V., Haynes, A.K., Brown, R.J., Thurston, J.B., and Lyatsky, V.B.
1992a: Aeromagnetic horizontal-gradient vector map of the Queen Charlotte Basin area, British Columbia. Geological Survey of Canada, Open File 2436.

Lyatsky, H.V., Thurston, J.B., Brown, R.J., and Lyatsky, V.B.
1992b: Hydrocarbon-exploration applications of potential-field horizontal gradient vector maps. Canadian Society of Exploration Geophysicists, Recorder, v.XVII, no.9, p.10-15

Miles, W., Stone, P.E., and Thomas, M.D.
1997: Magnetic and gravity anomaly maps with interpreted Precambrian basement, Saskatchewan. Geological Survey of Canada, Open File 3488, 5 sheets, 1:1,500,000 scale

Nettleton, L.L.
1971: Elementary gravity and magnetics for Geologists and Seismologists. Society of Exploration Geophysicists, 121p.

Newitt, L.R. and Haines, G.V.
1990: Magnetic Inclination Chart of Canada 1990. Geological Survey of Canada, Canadian Geophysical Atlas, Map 9.

Osadetz, K.G., Snowdon, l..R., and Stasiuk, L.D.
1989: Association of enhanced hydrocarbon generation and crustal structure in the Canadian Williston Basin. In; Current Research Part D, Geological Survey of Canada, Paper 89-1D, p.35-47.

Peirce, J.W., Charters, R.A., and Goussev,S.A.
1997: Magnetization of the Hines Creek Fault - an aeromagnetic case history. CSPG-SEPM 1997 Joint Convention, Calgary, Program with Abstracts, p.217.

Potter, D. and St. Onge, A.
1991: Minton Pool, south-central Saskatchewan: a model for basement induced structural and stratigraphic relationships. In; Proceedings of the Sixth International Williston Basin Symposium (J. Christopher and F. Haidl, eds.), p. 21-33.

Ross, G.M., Broome, J., and Miles, W.
1994a: Potential fields and basement structure in the Western Canada Sedimentary Basin. In; Geologic Atlas of the Western Canada Sedimentary Basin (G. Mossop and I. Shetson, comps.), p.41-47.

Ross, G.M., Mariano, J., and Dumont, R.
1994b: Was Eocene magmatism widespread in the subsurface of southern Alberta? Evidence from

new aeromagnetic data. In; Alberta Basement Transects, Lithoprobe Report 37 (G. Ross, ed.), p.240-249.

Reynolds, R.L., Rosenbaum, J.G., Hudson, M.R., and Fishman, N.S.
1990: Rock magnetism, the distribution of magnetic minerals in the Earth's crust and aeromagnetic anomalies. In; Geologic Applications of Modern Aeromagnetic Surveys (W. Hanna, ed.), USGS Bulletin 1924, p.24-25.

Sharpton, V.L., Grieve, R.A.F., Thomas, M.D., and Halpenny, J.F.
1987: Horizontal gravity gradient: an aid to the identification of crustal structure in North America. Geophysical Research Letters 14, p.808-811.

Sprenke, K.F., Wavra, C.S., and Godfrey, J.D.
1986: Geophysical expression of the Canadian Shield of northeastern Alberta. Alberta Research Council, Bulletin 52.

Thomas, M.D., Sharpton, V.L., and Grieve, R.A.F.
1987: Gravity patterns and Precambrian structure in the North American Central Plains. Geology, v.15, p.489-492.

Thomas, M.D. and Tanczyk, E.I.
1994: Progress in gravity and magnetic analysis along the Lithoprobe Trans-Hudson Orogen Transect. In; Trans-Hudson Orogen Transect, Lithoprobe Report 38 (Z.Hajnal and J.Lewry, eds.), p.135-150.

Thurston, J.B.
1991: Polynomial filtering of gravity data. MSC Thesis, Department of Geology and Geophysics, University of Calgary, 130p.

Thurston, J.B. and Brown, R.J.
1994: Automated source-edge location with a new variable-pass horizontal-gradient operator. Geophysics, v.59, p.546-554.

Weber, W.
1990: The Churchill-Superior Boundary Zone, southeast margin of the Trans-Hudson Orogen: a review. In; The Early Proterozoic Trans-Hudson Orogen of North America (J.Lewry and M.Stauffer, eds.). Geological Association of Canada, Special Paper 37, p.41-55.

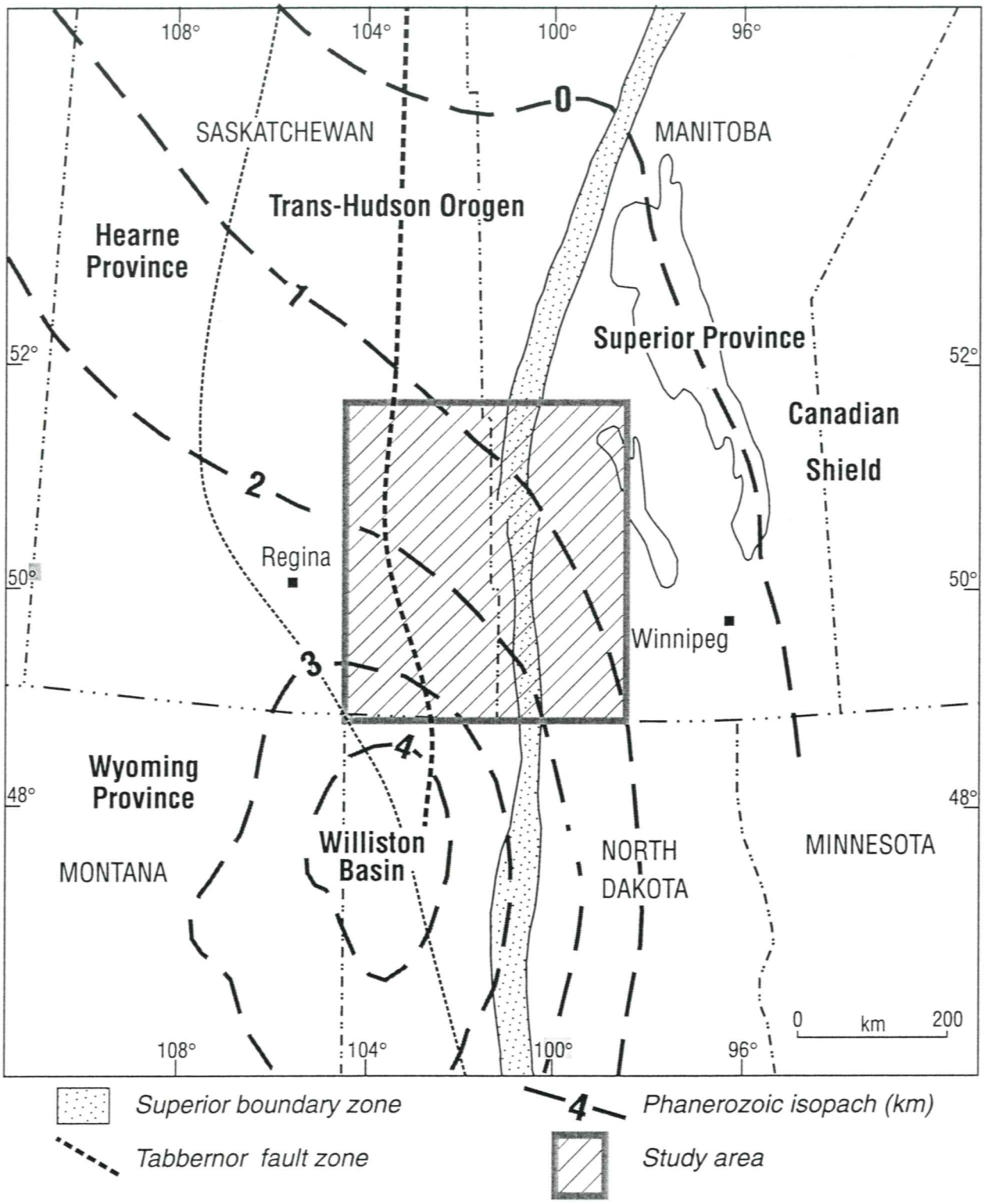

Figure 1. Location of study area in relation to Precambrian tectonic provinces and Phanerozoic Williston Basin. Locations of Churchill-Superior boundary zone and Tabbernor fault zone modified from Green et al. (1985) and Klasner and King (1986), to reflect the results of this study.

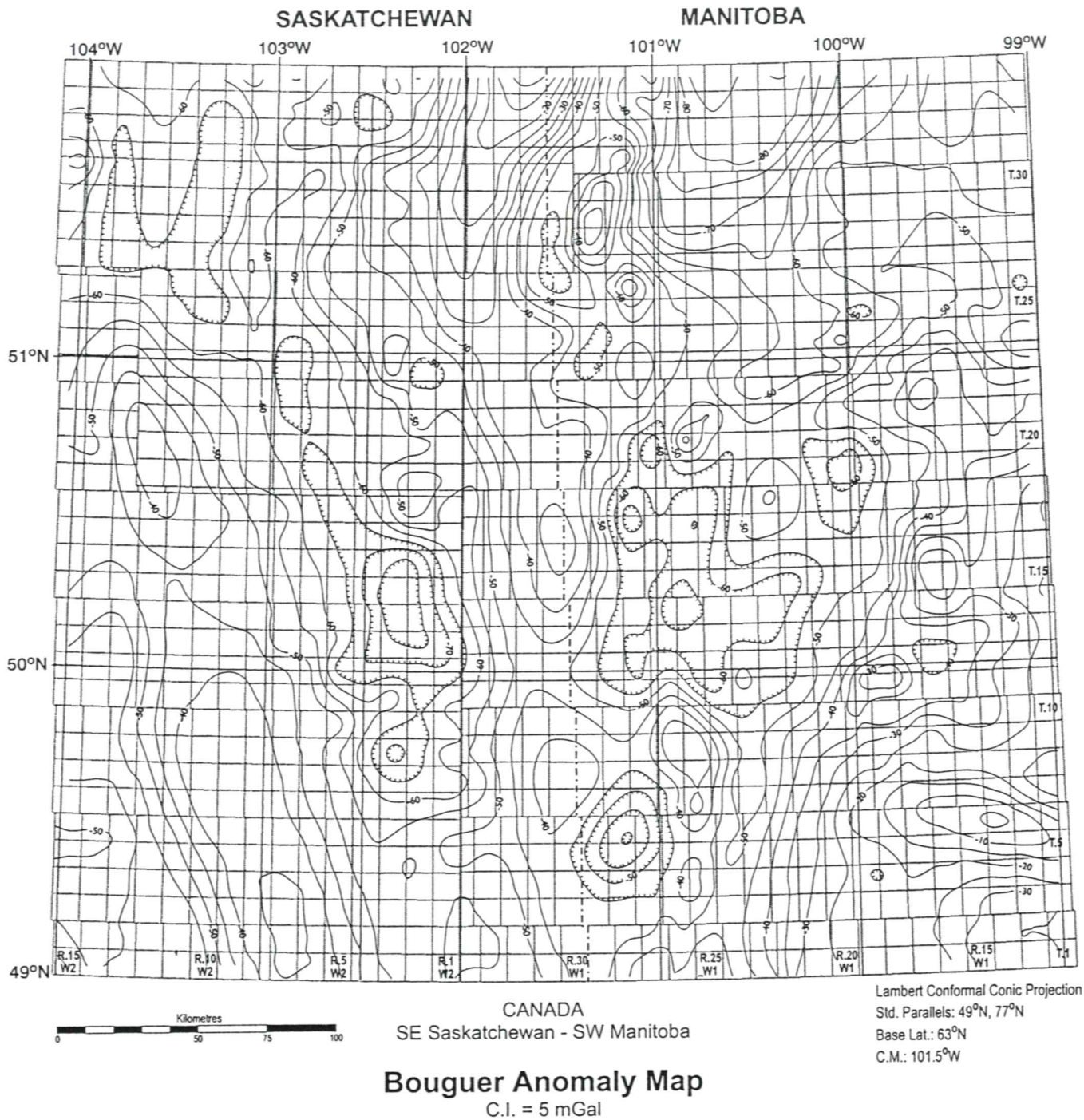

Figure 2. Bouguer gravity anomaly map of the study area; contour interval 5 mGal.

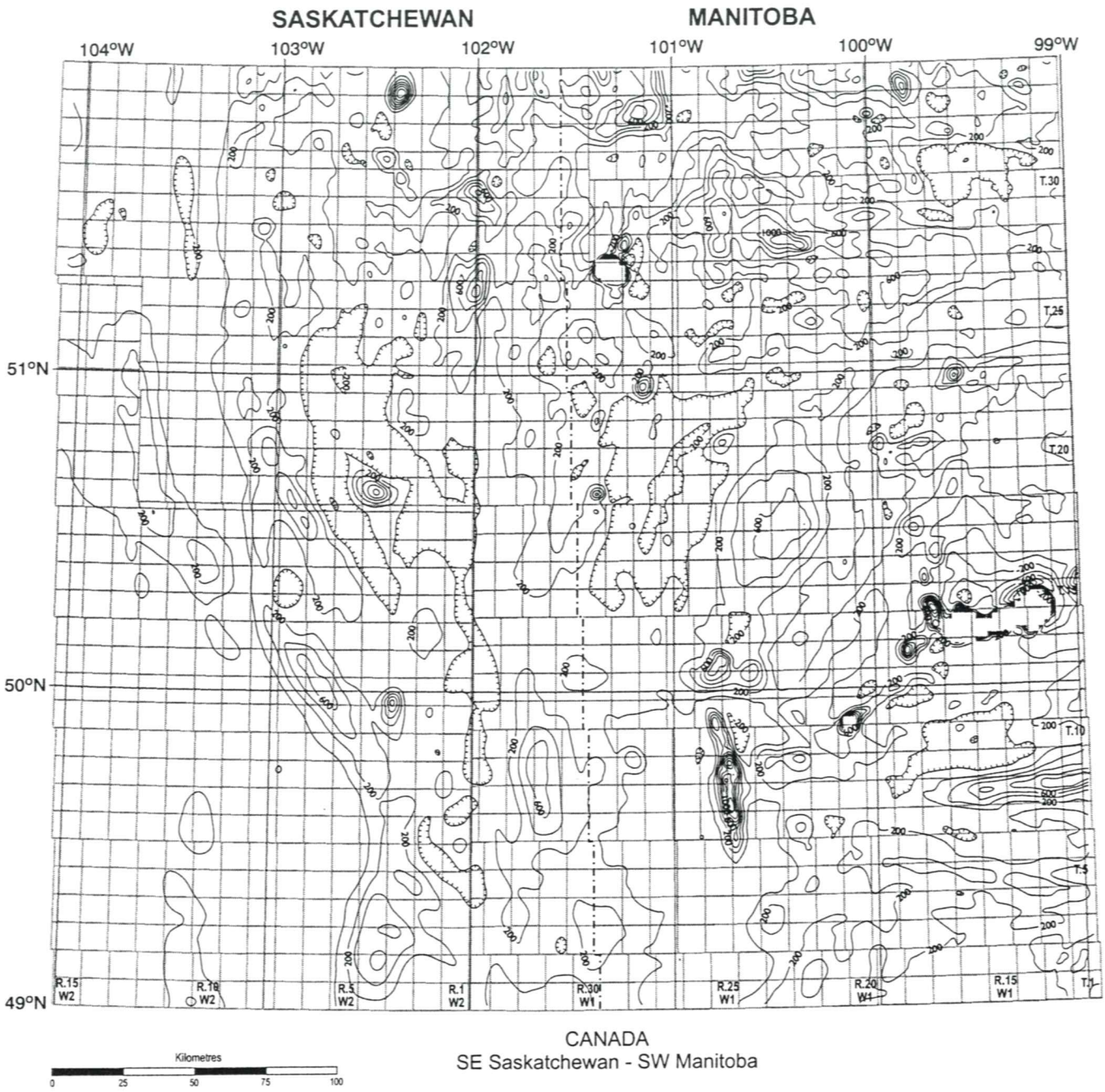

Figure 3. Total-field aeromagnetic anomaly map of the study area; contour interval 200 nT. Parts of three high-amplitude anomalies appear as rectangular blank areas, as some data points have been deleted to avoid contour overplotting.

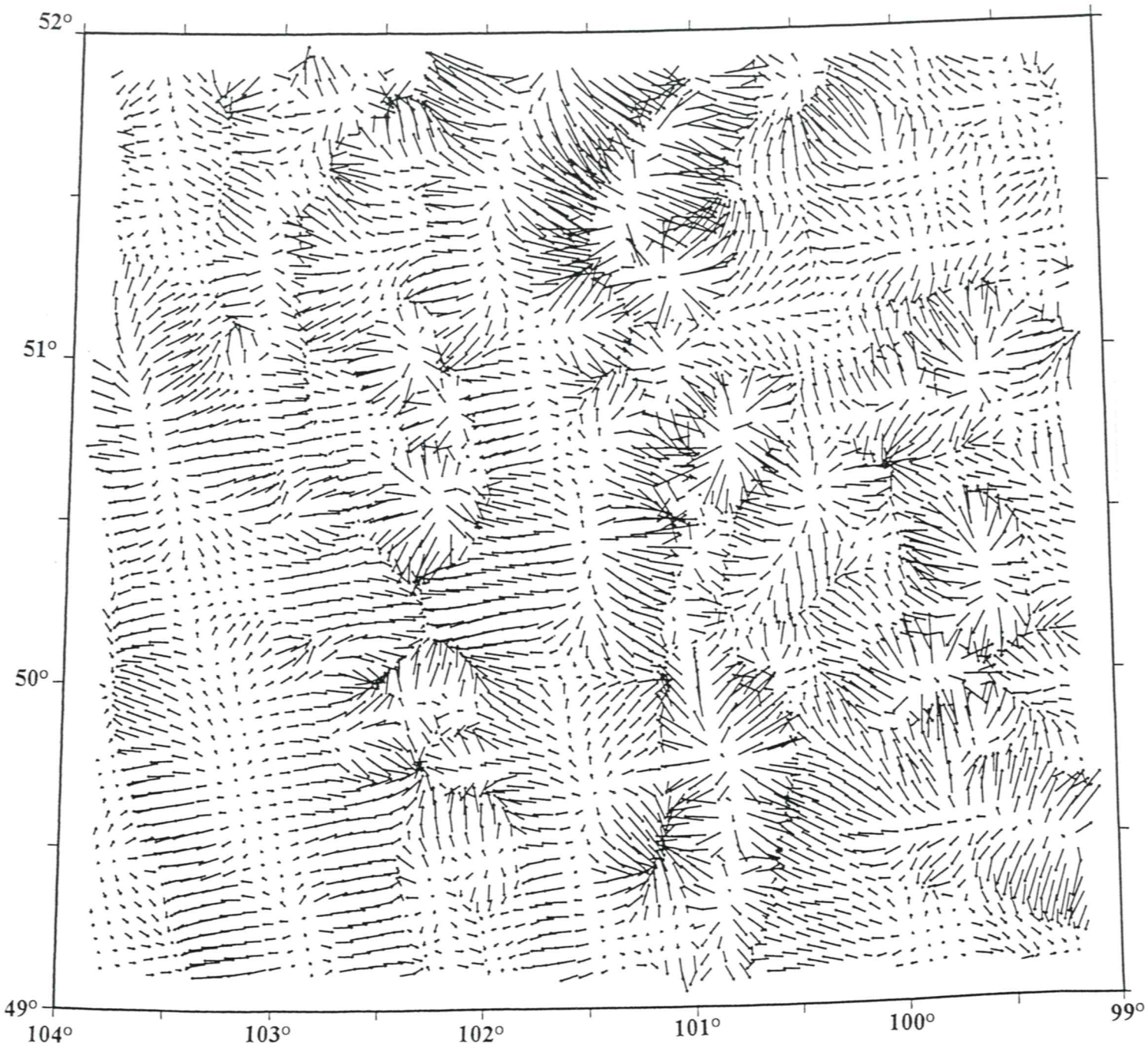

Figure 4. Gravity anomaly HGV map, derived from data gridded at a 5-km interval; arrows point downhill, linear scaling factor 0.5.

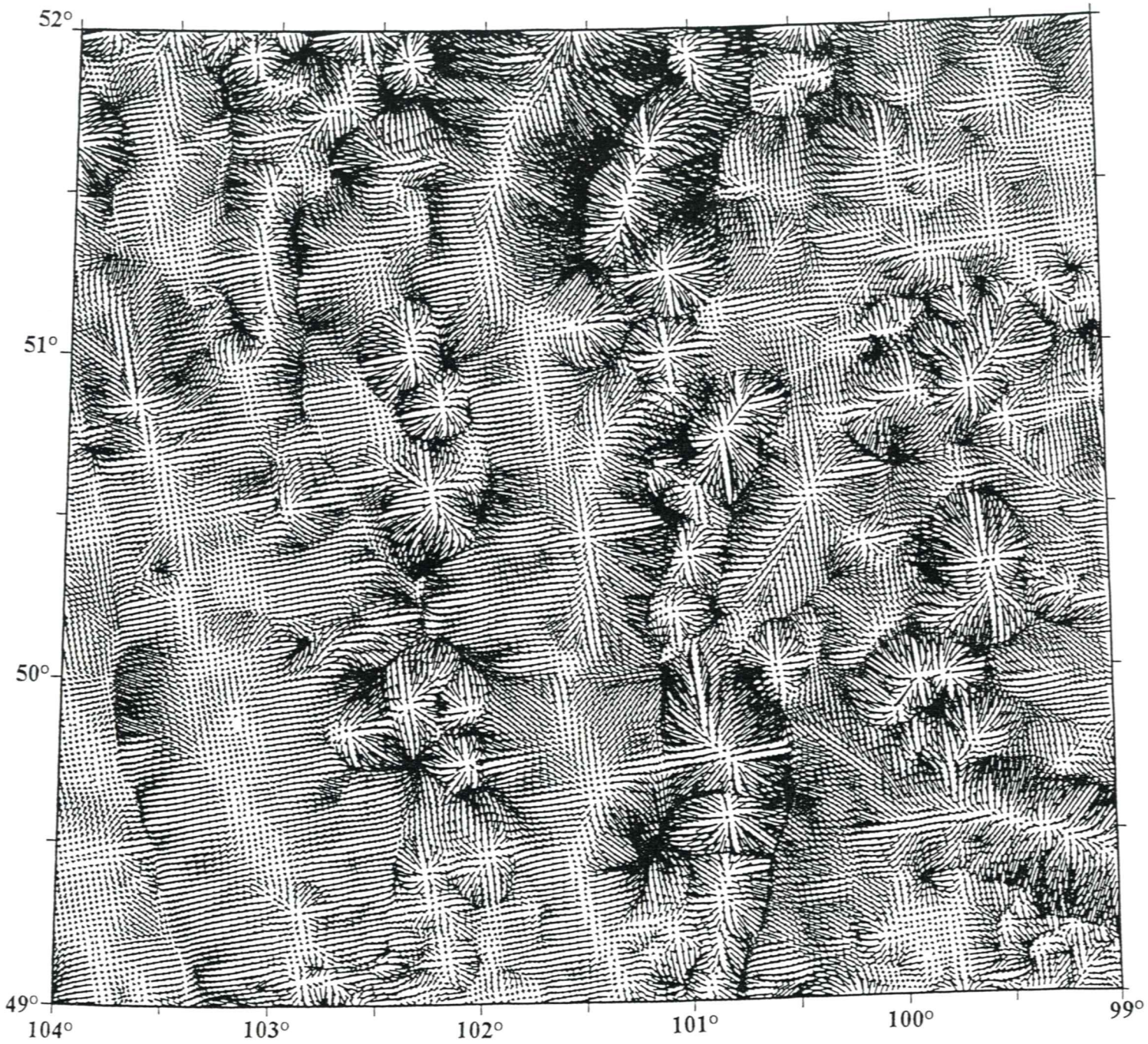

Figure 5. Gravity anomaly HGV map, derived from data gridded at a 2-km interval; arrows point downhill, linear scaling factor 0.5.

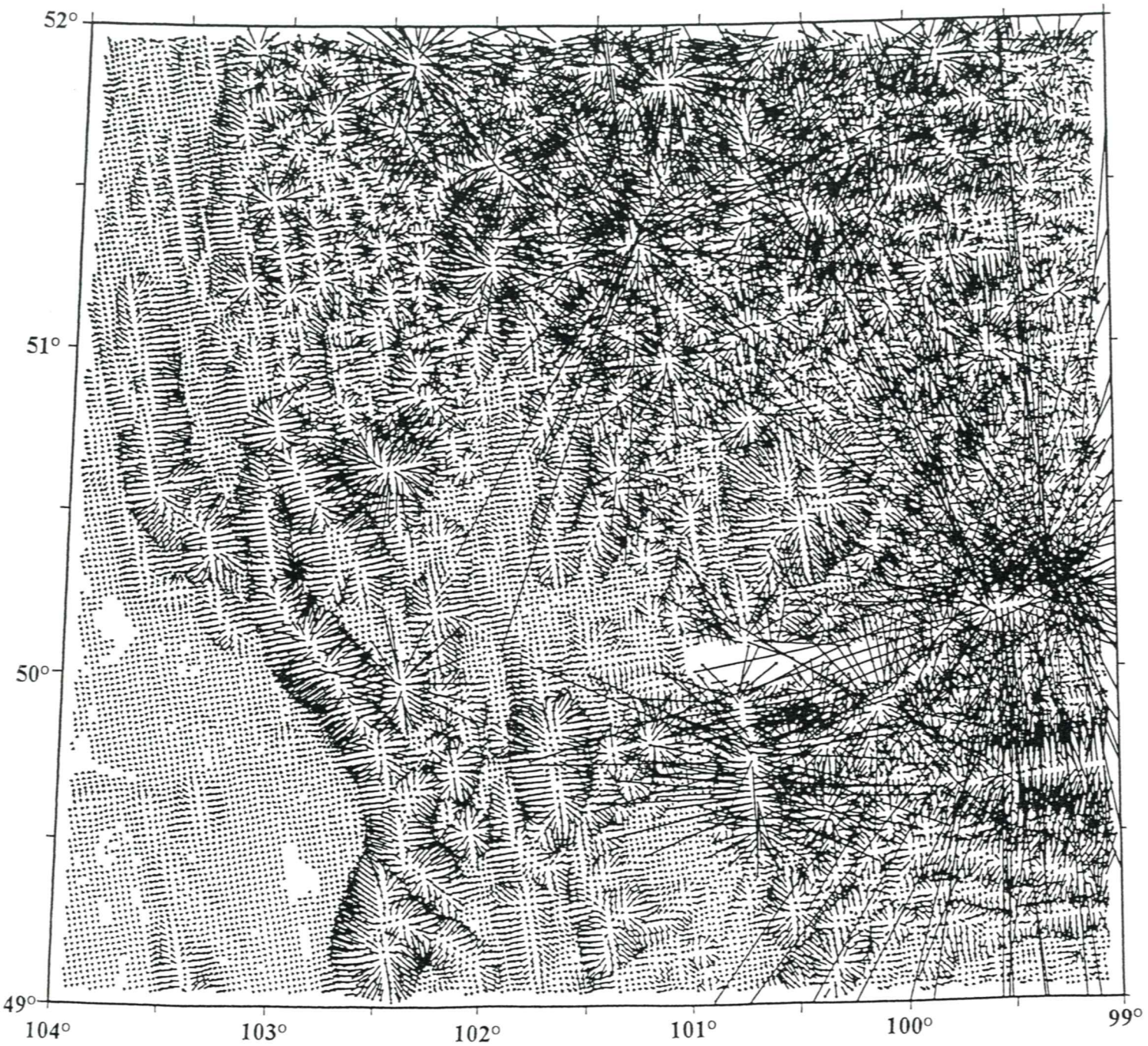

Figure 6. Magnetic anomaly HGV map, arrows point downhill, linear scaling factor 6.0.

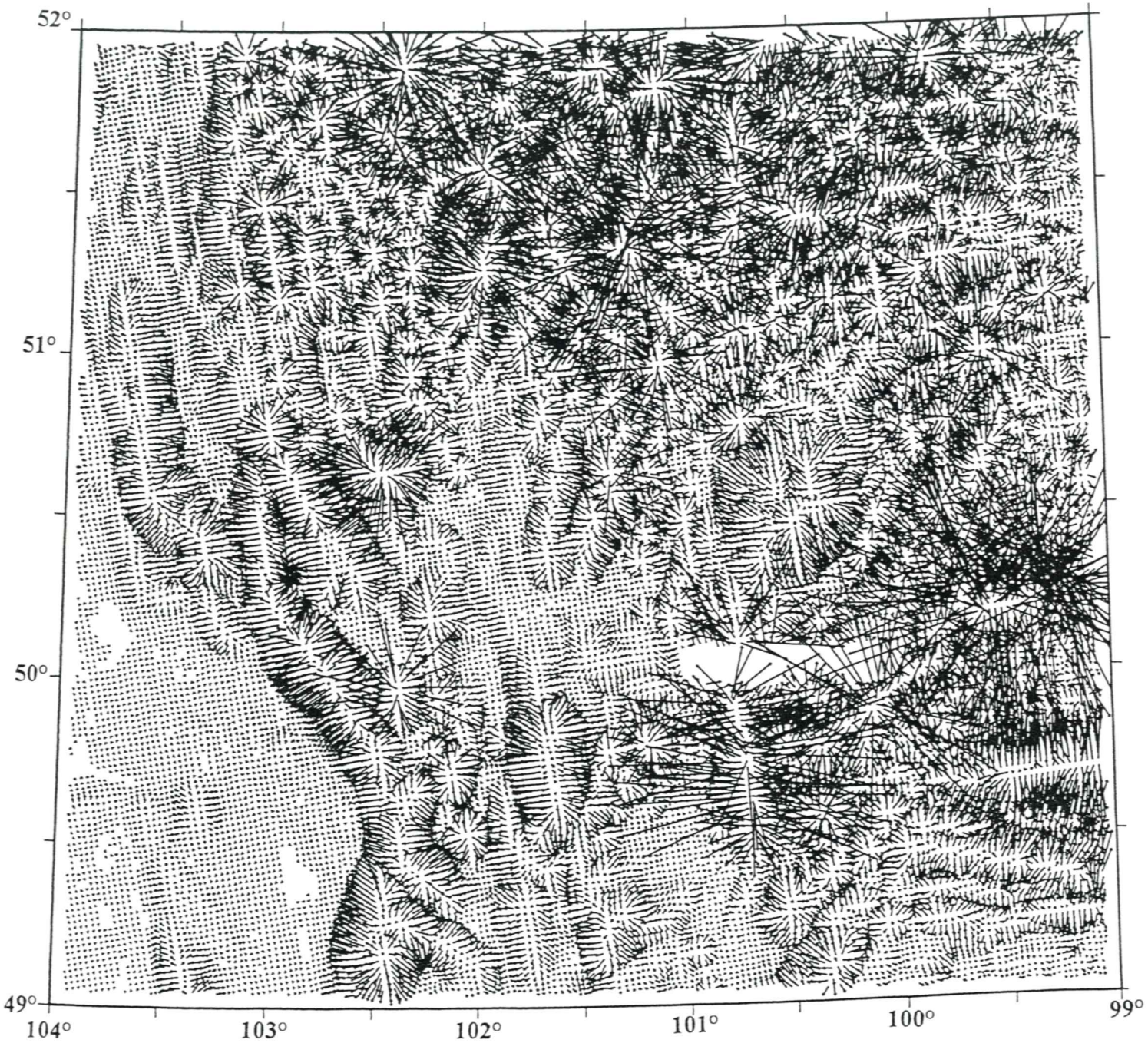

Figure 7. Magnetic anomaly HGV map, arrows point downhill, linear scaling factor 6.0, clipped at 15% of the maximum arrow length.

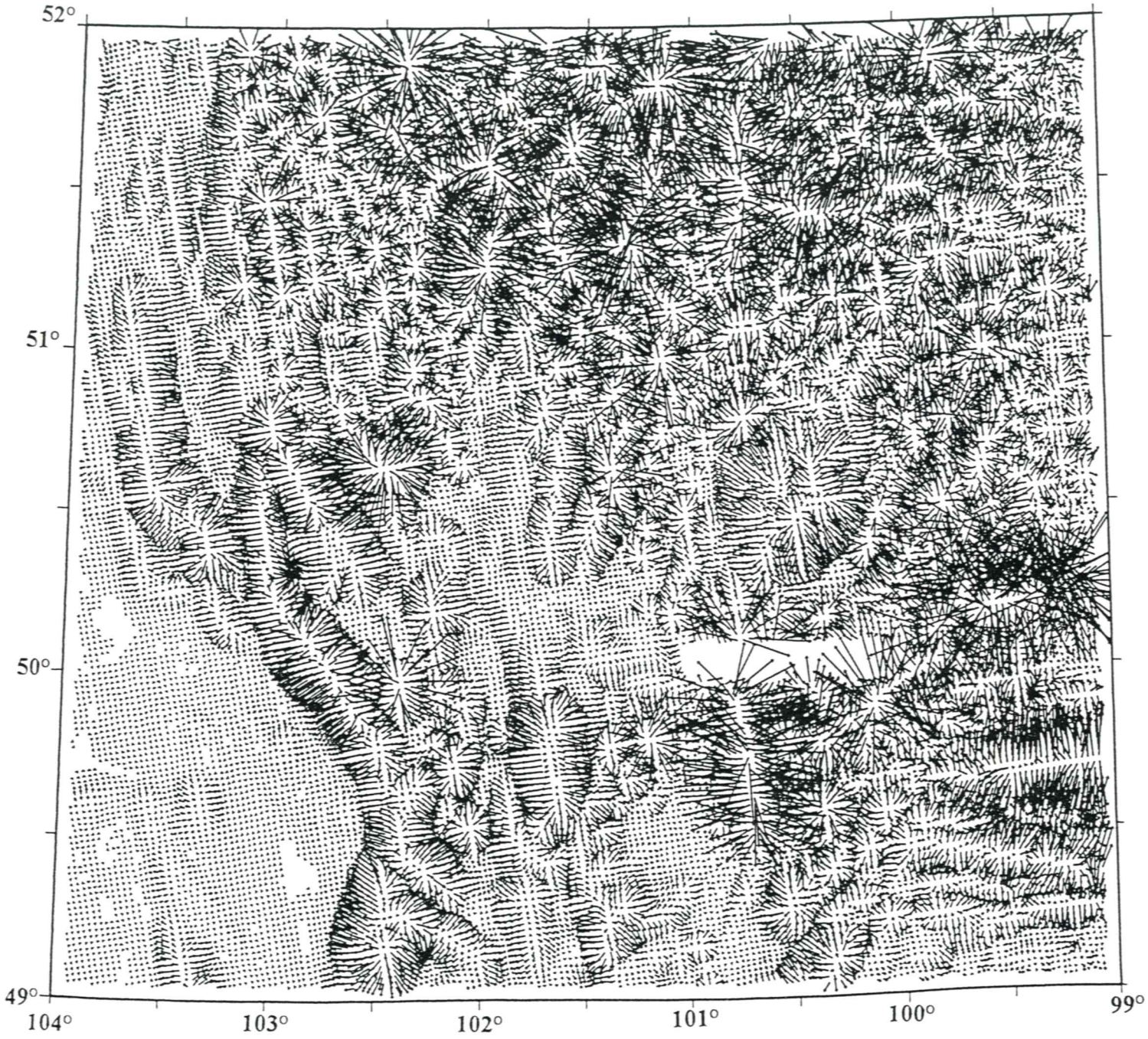

Figure 8. Magnetic anomaly HGV map, arrows point downhill, linear scaling factor 6.0, clipped at 7% of the maximum arrow length.

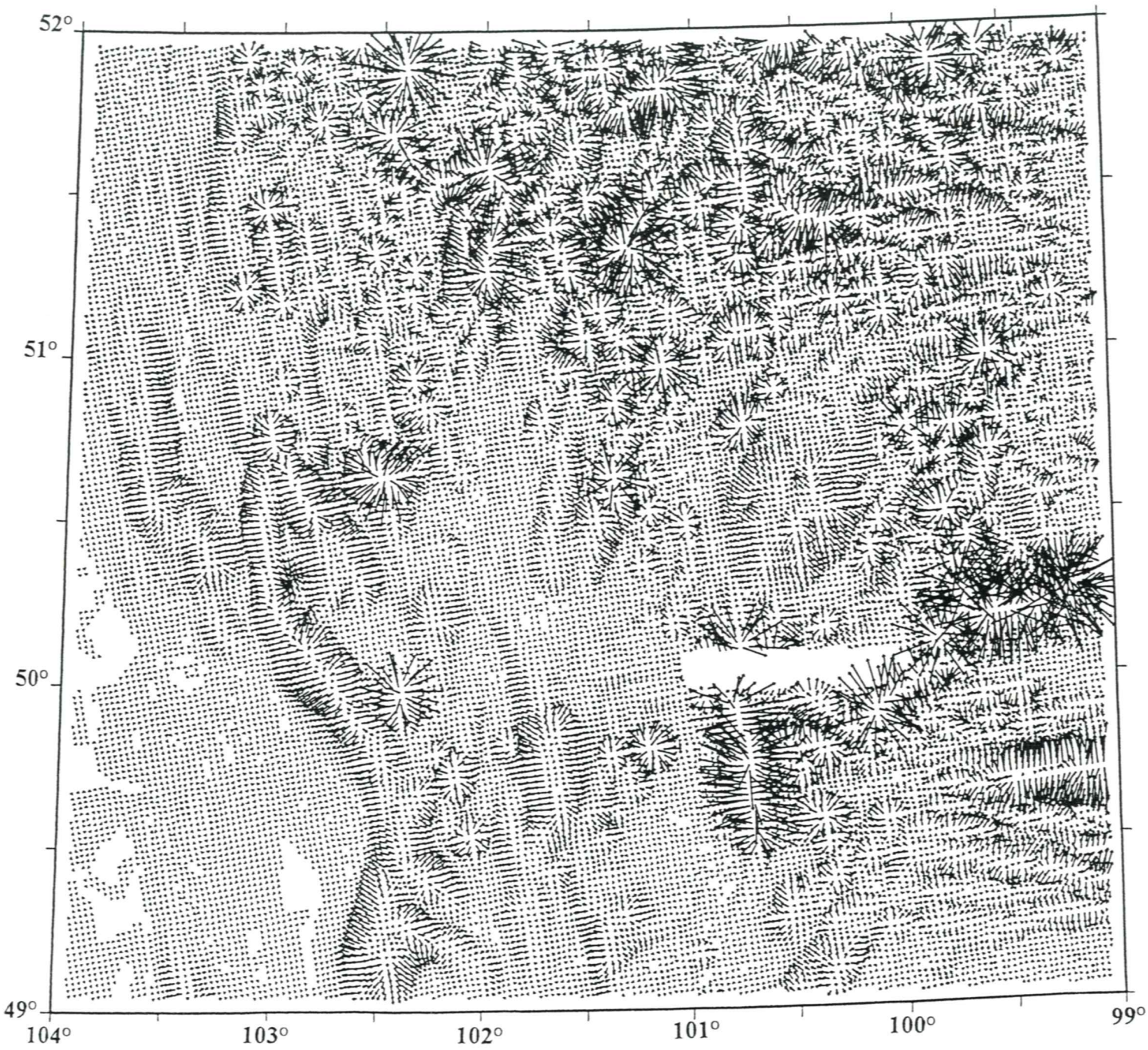

Figure 9. Magnetic anomaly HGV map, arrows point downhill, linear scaling factor 3.0, clipped at 9% of the maximum arrow length.

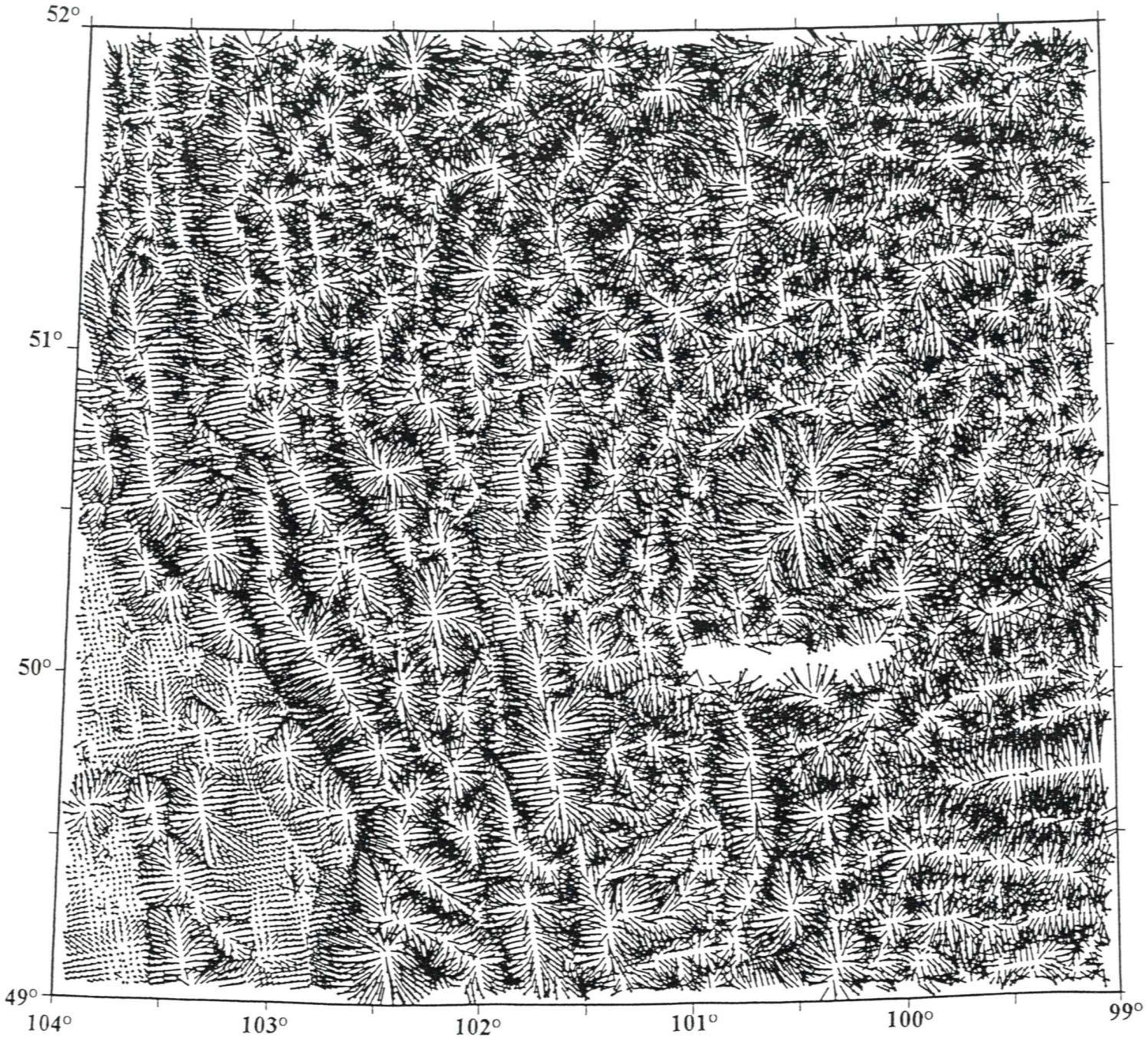

Figure 10. Magnetic anomaly HGV map, arrows point downhill, logarithmic scaling factor 0.3.

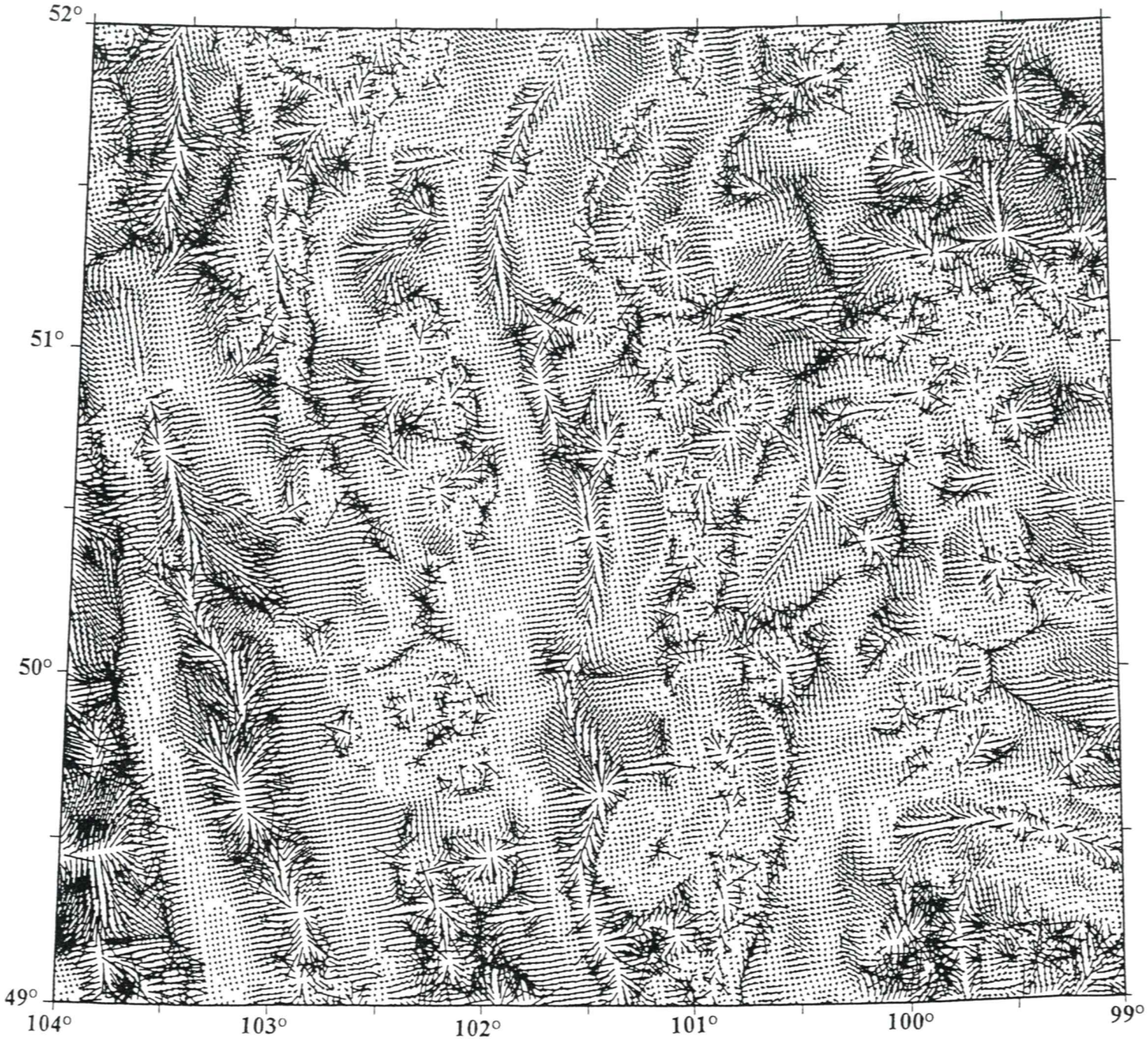

Figure 11. Gravity anomaly HGV map, arrows point downhill, logarithmic scaling factor 0.1.

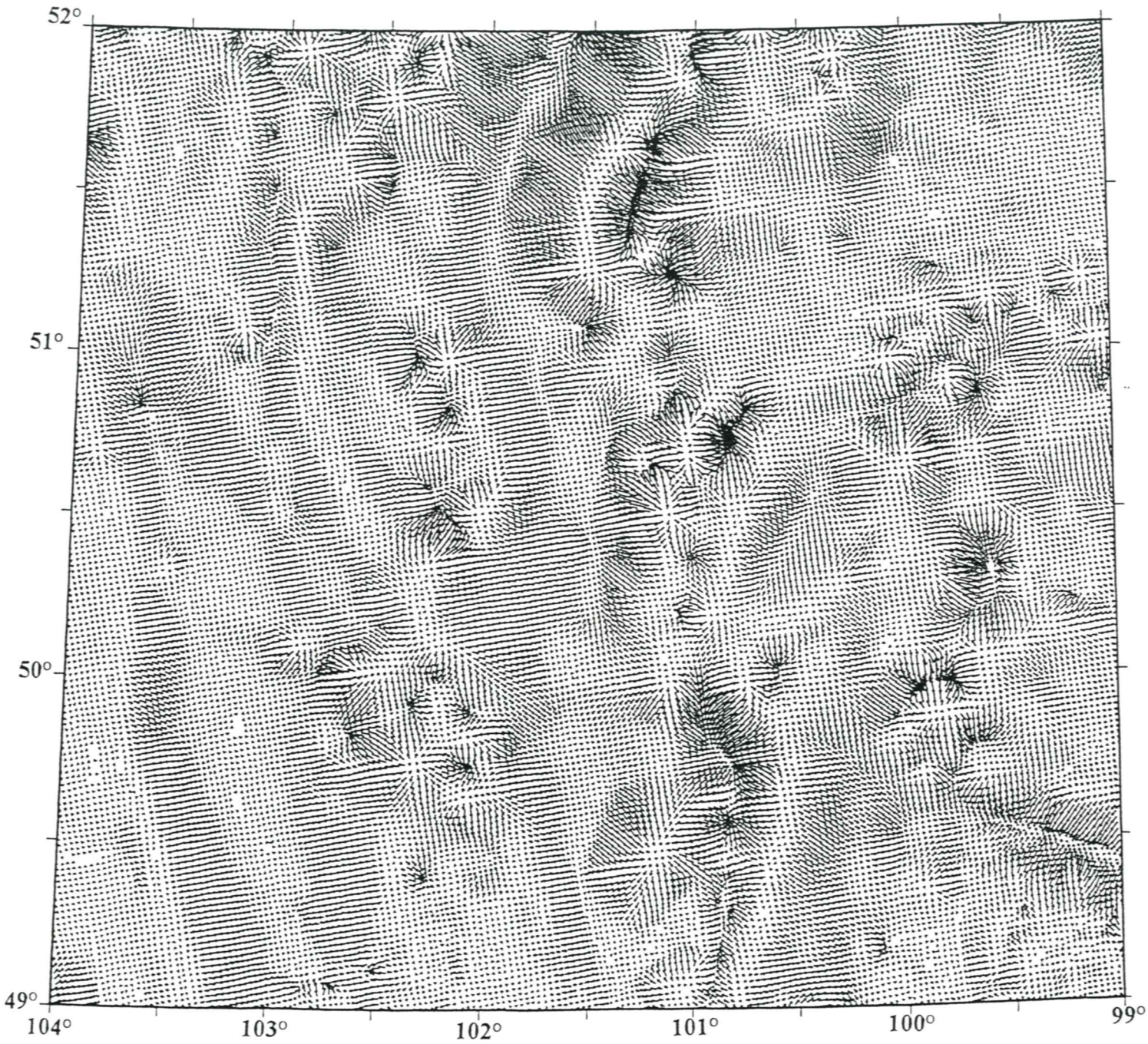

Figure 12. Gravity anomaly HGV map, arrows point uphill, linear scaling factor 0.2.

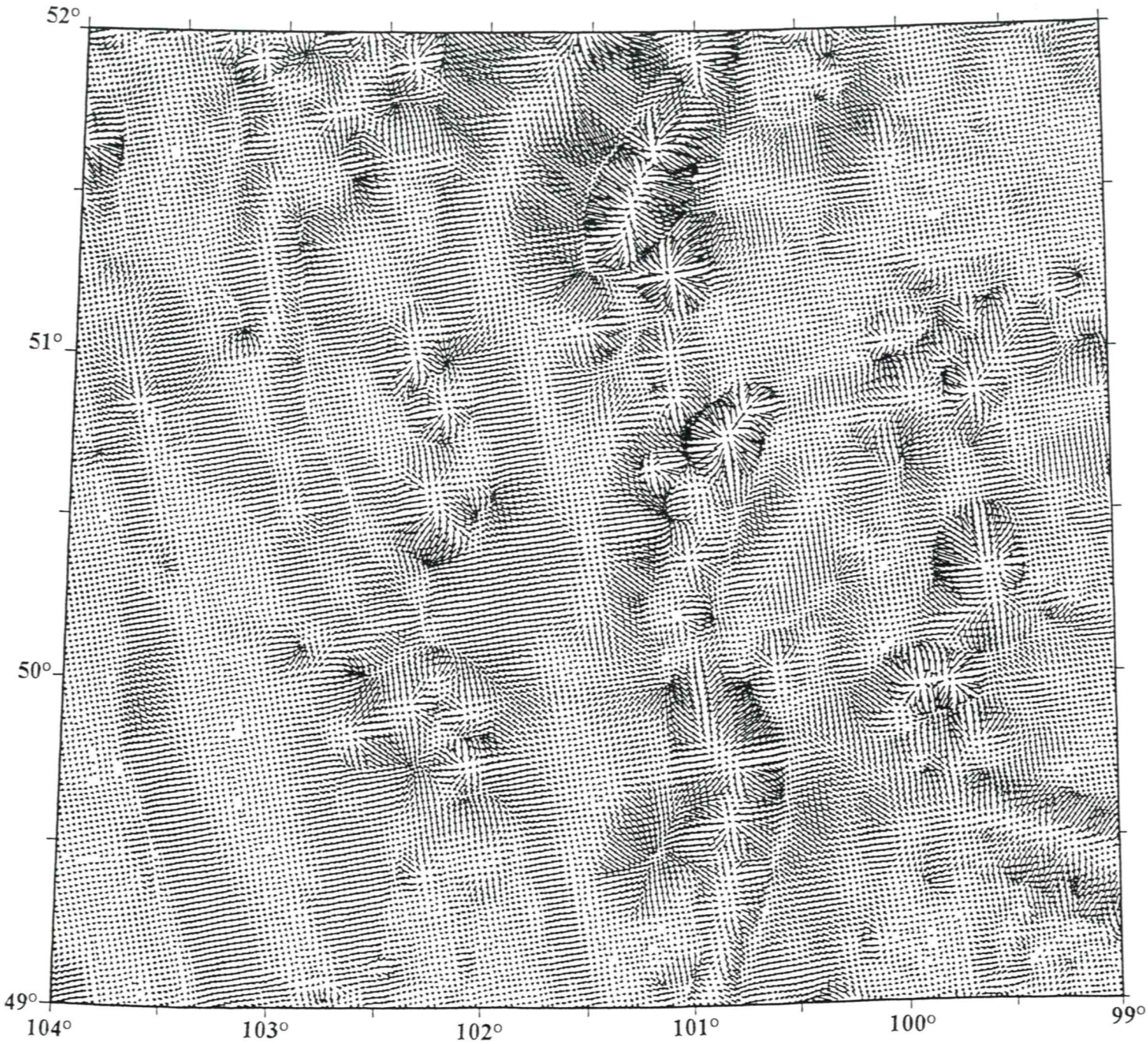

Figure 13. Gravity anomaly HGV map, arrows point downhill, linear scaling factor 0.2.

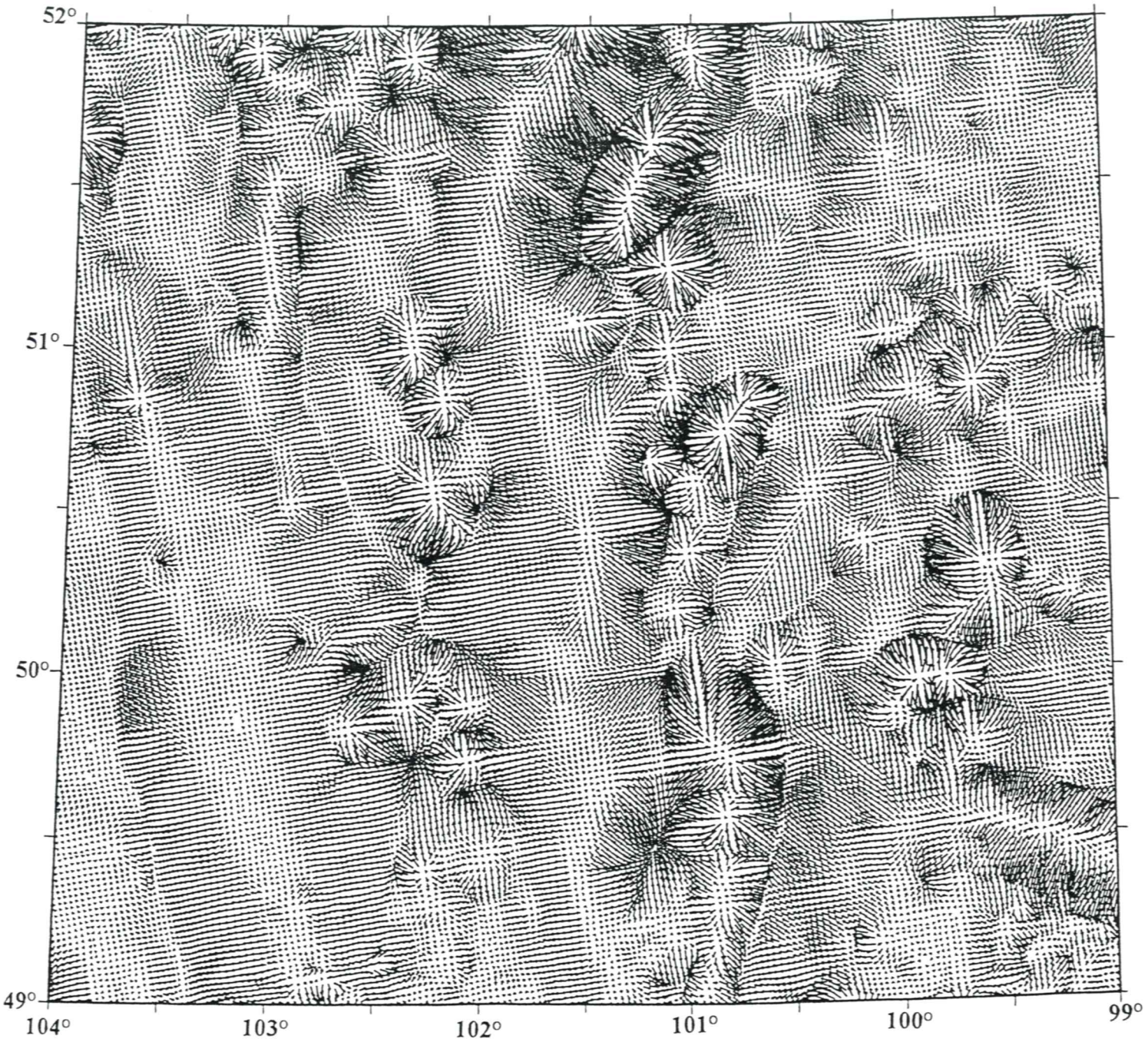

Figure 14. Gravity anomaly HGV map, arrows point downhill, linear scaling factor 0.3.

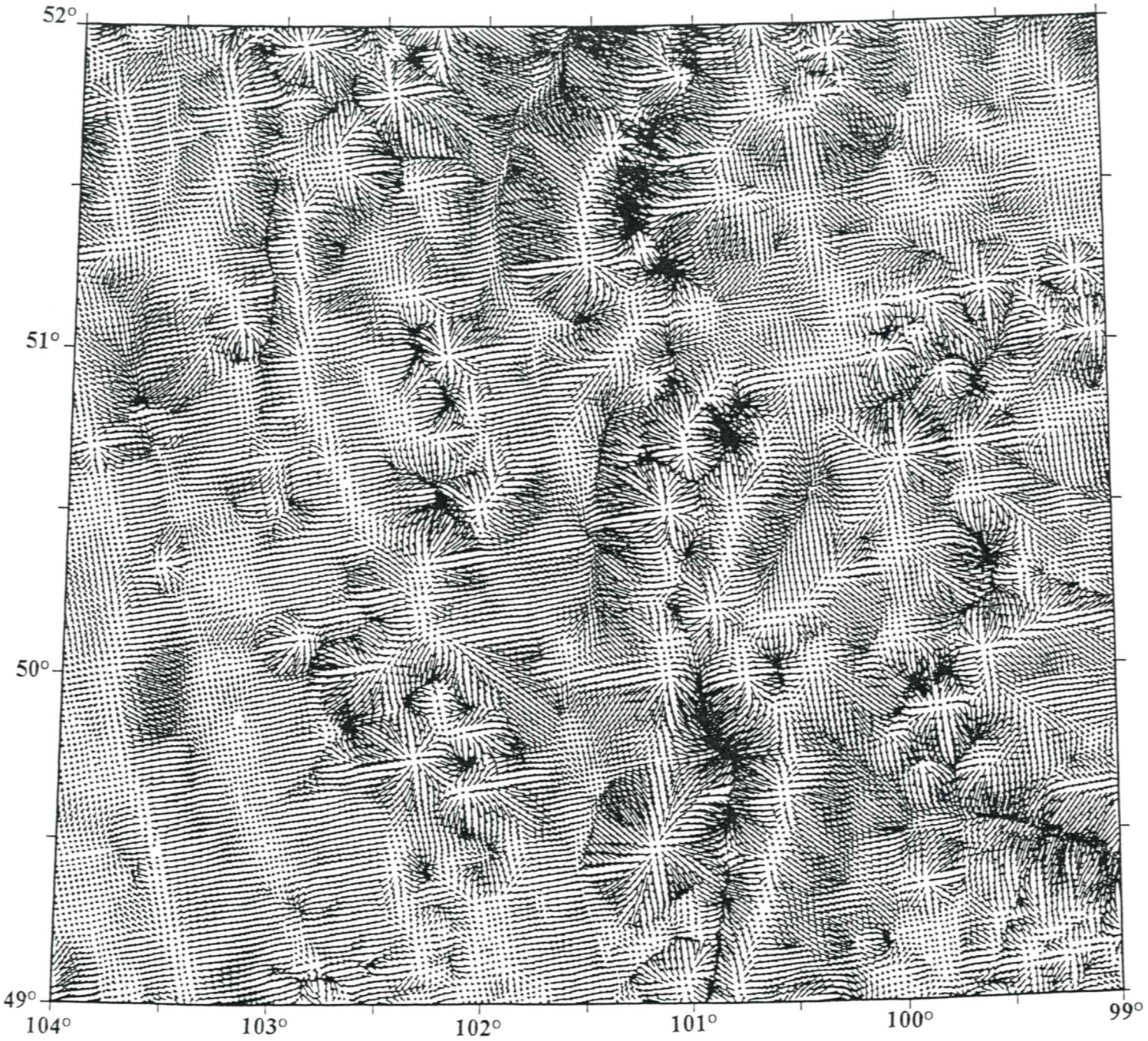

Figure 15. Gravity anomaly HGV map, arrows point uphill, linear scaling factor 0.4.

Figure 16. Gravity anomaly HGV map, arrows point uphill, linear scaling factor 0.6.

Figure 17. Gravity anomaly HGV map, arrows point downhill, linear scaling factor 0.6.

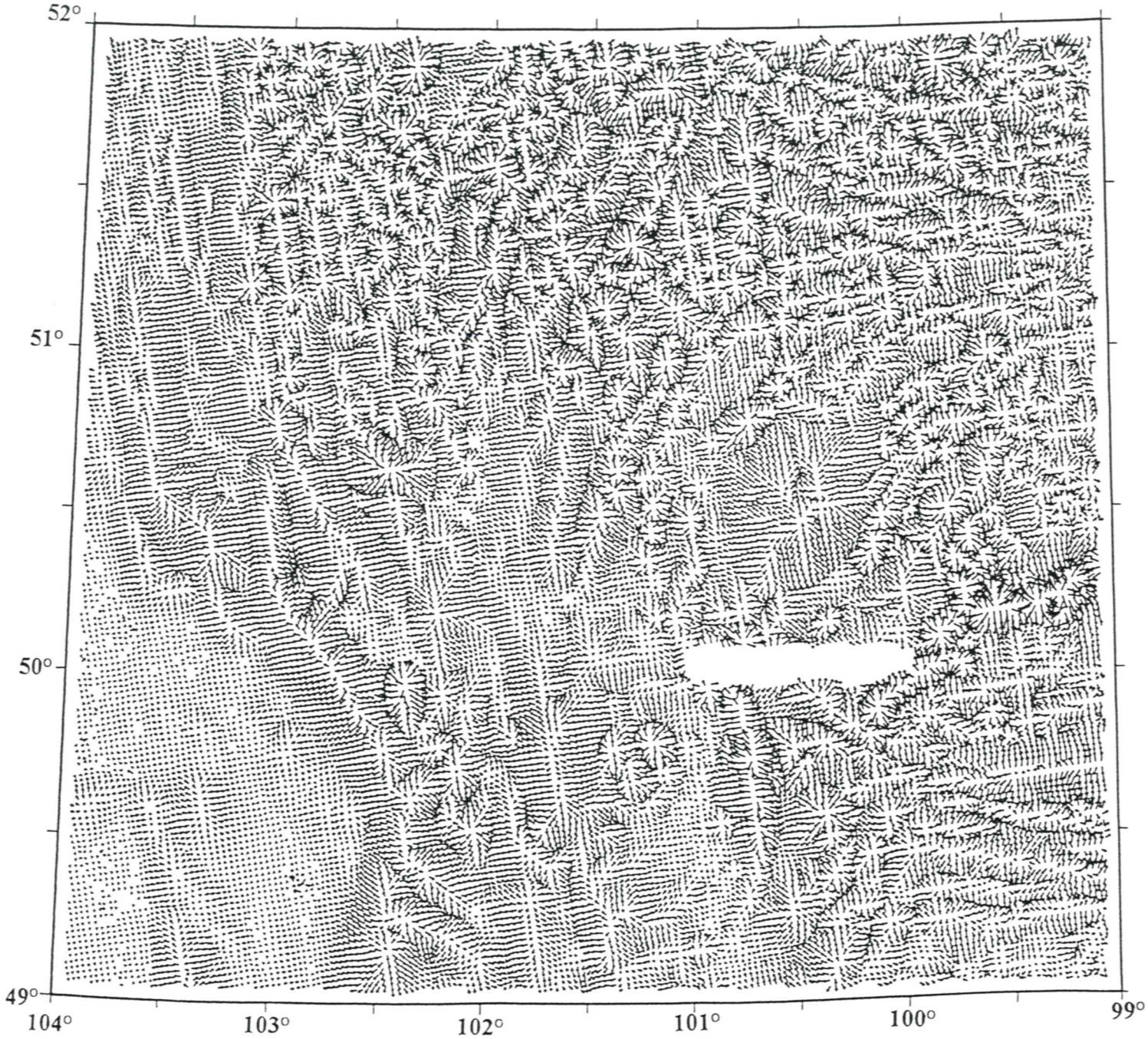

Figure 18. Magnetic anomaly HGV map, arrows point downhill, logarithmic scaling factor 0.1.

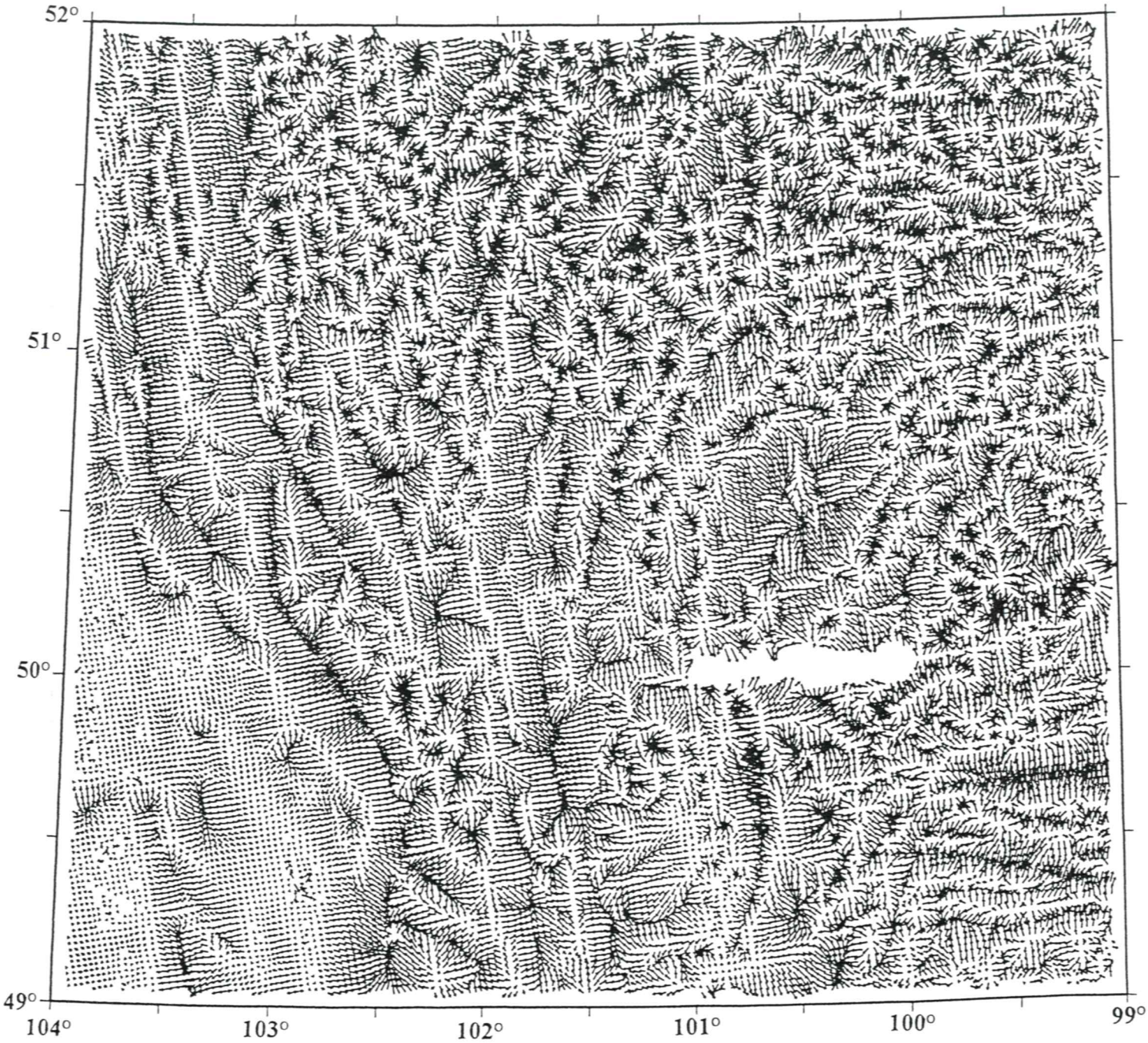

Figure 19. Magnetic anomaly HGV map, arrows point uphill, logarithmic scaling factor 0.15.

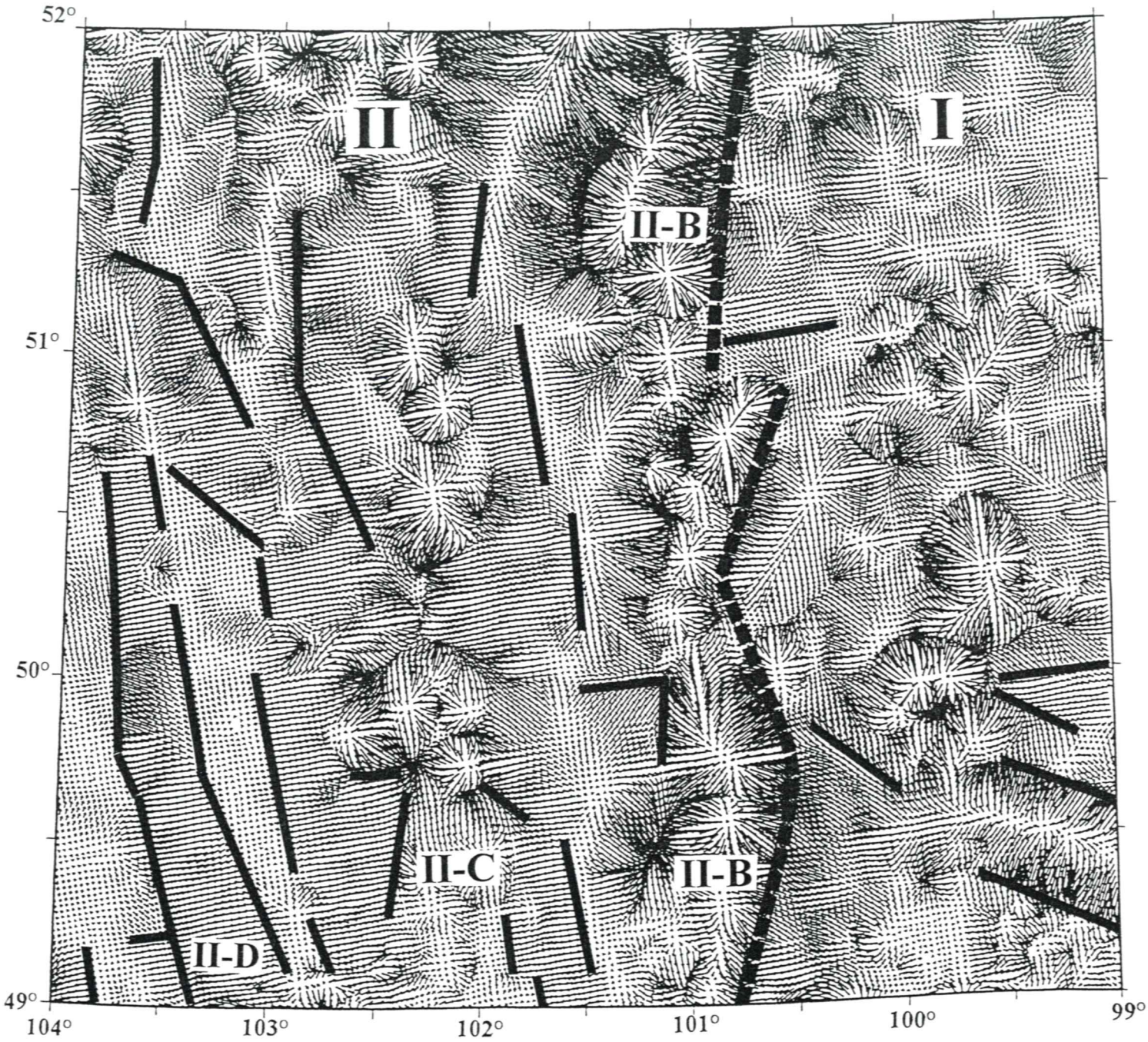

Figure 20. Gravity anomaly HGV map (arrows point downhill, linear scaling) with interpreted anomaly domains I and II, and anomaly features II-B, II-C and II-D. Heavy dashed line indicates position of domain I-II boundary; solid line segments indicate HGV lineaments, many of which may be associated with crustal block edges.

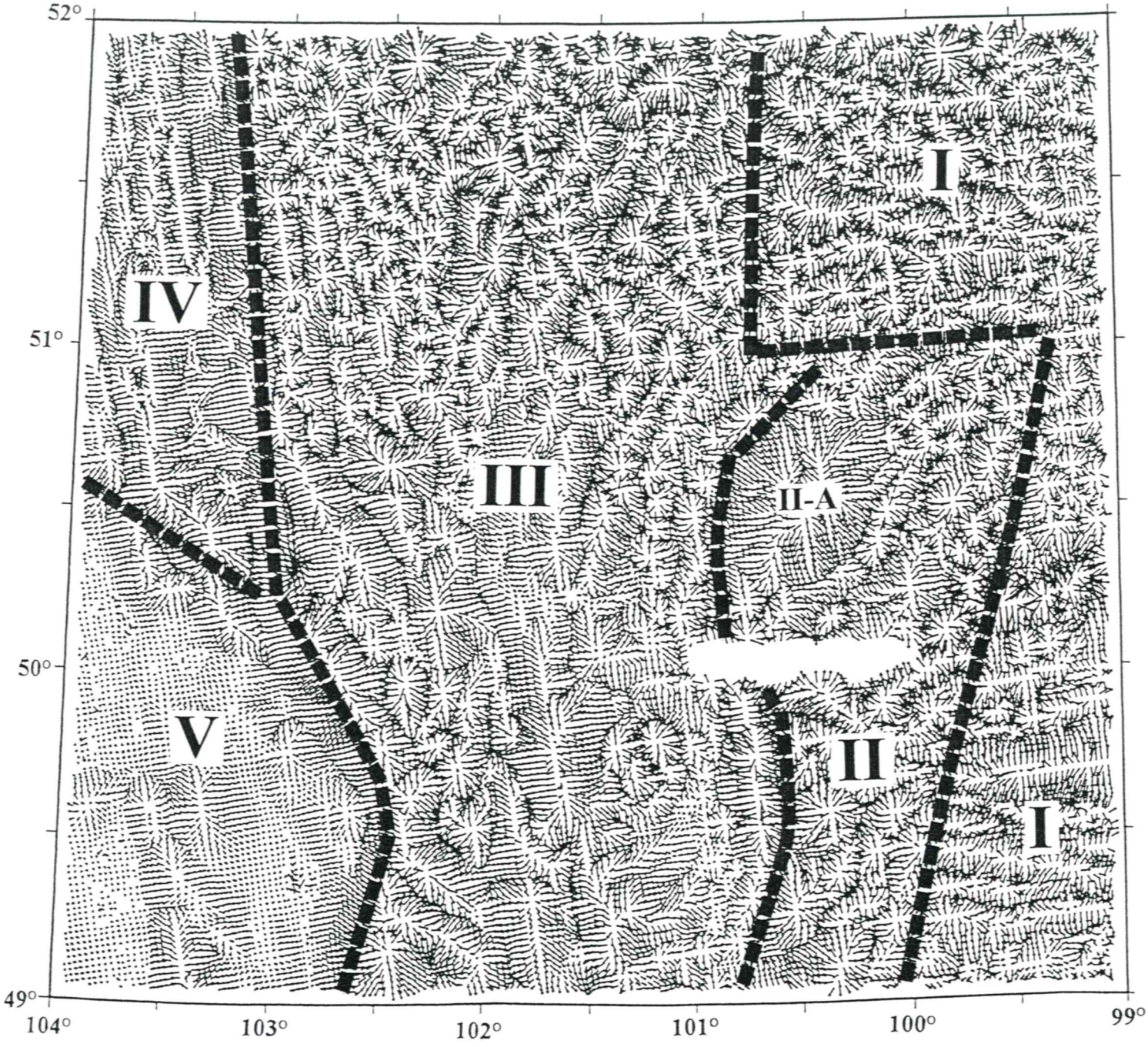

Figure 21. Magnetic anomaly HGV map (arrows point downhill, logarithmic scaling) with interpreted anomaly domains I to V (boundaries indicated by dashed lines) and anomaly feature II-A

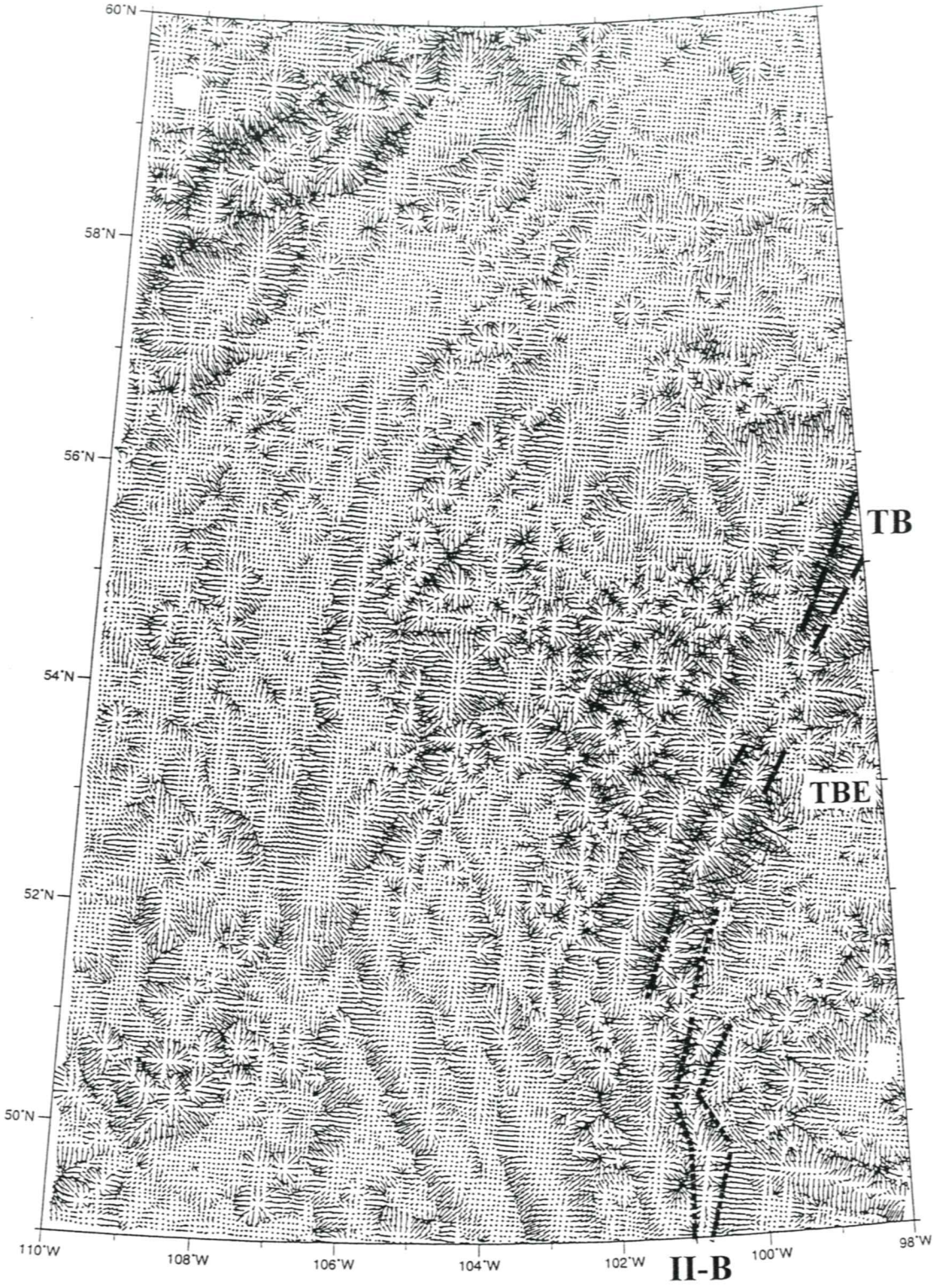

Figure 22. Regional gravity anomaly HGV map (arrows point downhill, linear scaling) of Saskatchewan and western Manitoba, with indicated positions of Thompson Belt (TB) in the Canadian Shield (adapted from Thomas and Tancyzk, 1994), the Thompson Belt extension (TBE) south of the Shield margin (adapted from Lucas et al., 1996), and the gravity II-B anomaly trend (described in this study).